LA-13739-MS

Approved for public release;
distribution is unlimited.

Interaction of Plutonium with Diverse Materials in Moist Air and Nitrogen-Argon Atmospheres at Room Temperature

Los Alamos
NATIONAL LABORATORY

Los Alamos National Laboratory is operated by the University of California for the United States Department of Energy under contract W-7405-ENG-36.

Edited by Lynne Atencio, Group IM-1

An Affirmative Action/Equal Opportunity Employer

LA-13739-MS

Issued: April 2001

Interaction of Plutonium with Diverse Materials in Moist Air and Nitrogen-Argon Atmospheres at Room Temperature

*John M. Haschke**
Raymond J. Martinez
Robert E. Pruner II
Barbara Martinez
Thomas H. Allen

**Guest Scientist to NMT-DO, Seaborg Institute, 11003 Willow Bend Drive, Waco, TX 76712.*

Los Alamos
NATIONAL LABORATORY
Los Alamos, New Mexico 87545

INTERACTION OF PLUTONIUM WITH DIVERSE MATERIALS IN MOIST AIR AND NITROGEN-ARGON ATMOSPHERES AT ROOM TEMPERATURE

John M. Haschke, Raymond J. Martinez, Robert E. Pruner II, Barbara Martinez, and Thomas H. Allen

ABSTRACT

Chemical and radiolytic interactions of weapons-grade plutonium with metallic, inorganic, and hydrogenous materials in atmospheres containing moist air-argon mixtures have been characterized at room temperature from pressure-volume-temperature and mass spectrometric measurements of the gas phase. A reaction sequence controlled by kinetics and gas-phase composition is defined by correlating observed and known reaction rates. In all cases, O_2 is eliminated first by the water-catalyzed Pu + O_2 reaction and H_2O is then consumed by the Pu + H_2O reaction, producing a gas mixture of N_2, argon, and H_2. Hydrogen formed by the reaction of water and concurrent radiolysis of hydrogenous materials either reacts to form PuH_2 or accumulates in the system. Accumulation of H_2 is correlated with the presence of hydrogenous materials in liquid and volatile forms that are readily distributed over the plutonium surface. Areal rates of radiolytic H_2 generation are determined and applied in showing that modest extents of H_2 production are expected for hydrogenous solids if the contact area with plutonium is limited. The unpredictable nature of complex chemical systems is demonstrated by occurrence of the chloride-catalyzed Pu + H_2O reaction in some tests and hydride-catalyzed nitriding in another.

Introduction

The chemical interaction of metallic plutonium with nonnuclear materials is an essential consideration for the extended storage of plutonium in sealed containers [1]. The possibility of containment failure is enhanced by reactions that generate internal pressure by expansion of the solid phase or by the formation of noncondensable gases. The occurrence of potentially

detrimental reactions is reduced by the exclusion of hydrogenous materials and water from the storage environment, as required by the DOE standard for the storage of metal and oxide [2]. The effectiveness of material stabilization procedures is uncertain, and compliance with the standard is difficult to verify, especially for plutonium-containing residues derived from diverse sources and containing unspecified constituents [1].

The present study was initiated in an effort to identify and determine the kinetics of reactions that occur when plutonium is exposed to a broad spectrum of potentially reactive materials. A test matrix was developed to investigate the chemical behavior of differing types of materials, including metals, inorganic compounds, water, and hydrogenous substances with complex, but well-defined, chemical compositions. As far as possible, liquid or fluid (slurry) test materials were selected in an effort to reduce uncertainties associated with the physical contact of the reactants with the plutonium surface. The dimension of the matrix was reduced by partially inserting the atmospheres into reaction vessels and allowing reactions to proceed until the oxygen and water were chemically eliminated from the systems. The chemical behavior in the residual nitrogen-argon atmospheres was then determined by extending the test period.

Results for hydrogenous materials in oxygen-containing atmospheres are of special interest because of their relevance to questions regarding the chemical fate of oxygen and water in plutonium storage containers [3]. The radiolytic generation of H_2 in tests with hydrogenous materials provides opportunities for investigating the chemical behavior of O_2 and H_2 mixtures in plutonium-containing systems. In addition, the study yields information on the chemical interaction of H_2O with plutonium and direct measurements of pressure-time (P-t) data for sealed vessels containing potentially reactive materials.

Experimental Methods

Interactions of test materials with plutonium were investigated using pressure-volume-temperature (PVT) techniques to monitor pressure changes in the gaseous atmosphere over time, and mass spectrometry (MS) to define gas-phase compositions. PVT results were used for determining reaction rates and correlating behavior with known reactions. MS results provided a reliable reference for confirming results and conclusions.

PVT measurements were made using stainless steel reactors (862 ± 1 cm^3 volume, 3.3 kg mass) with elastomeric O-ring closures. Each reactor was fitted with a valve and a pressure transducer calibrated for the 0–1000 torr range. Although initial pressures were consistent with ambient values (580 ± 8 torr), measured changes in pressure, resulting from the depletion of O_2 from the gas phase, were less than expected for the pressures and oxygen

concentrations in the initial test atmospheres. Further evaluations of the results indicated that the transducer calibrations were inaccurate and showed that pressure changes were less than the actual values by a factor of 1.76 ± 0.13; therefore, pressure-time data are presented as measured values, but corrected pressures are used for quantitative assessments.

Specimens of weapons-grade delta-phase plutonium were prepared by cutting squares from a metal sheet and forming them into cups by pressing them in a spherical-segment die set with a hydraulic press. The resulting cups had diameters of 4.5 cm, maximum depths of 1.3 cm, and volumes of approximately 8 cm^3. After the corners of the specimens were removed to facilitate their placement into the test reactors, their geometric surface areas were 80 ± 5 cm^2.

Each of the test materials listed in Table 1 was transferred into a plutonium cup that was positioned near the reactor opening on a cylindrical stainless steel stand. Cellular silicone, the only test material initially present as a solid, was held in contact with the plutonium surface by filling the cup with stainless steel shot. Photographs of the cups and the loaded test materials were taken before the reactors were closed. The sealed reactors were partially purged by repeatedly pressurizing the reactors with argon and venting them until a mixture containing about 50% argon and 50% air remained. The chemical compositions of the test materials are given in Table 2. The initial compositions of the gas phase in Table 3 were calculated using the N_2:Ar ratio determined from MS data for the final gas mixtures and the known molar ratios of constituents in air.

Chemical behavior at 23 ± 2°C was monitored by measuring pressure as a function of time and by determining the final gas composition by MS analysis. The P-t data for the time period between 0.7 and 2 years were lost because the record became contaminated with plutonium during an accidental release into the laboratory. Upon termination of the tests after 3.3 years, residual gases were analyzed, the plutonium specimens were weighed, and solid products were photographed. A product formed by the interaction of Indalloy 51 with plutonium was submitted for characterization by metallography, x-ray diffraction (XRD), and scanning electron microscopy (SEM) analysis. Reaction rates derived from the slopes of P-t curves and geometric areas of plutonium specimens are reported in units of mol/cm^2 min.

Table 1. Summary of Test Conditions

Test Material	Reactor Volume (cm^3)	Mass of Pu (g)	Mass of Test Material (g)	Initial Pressure (torr)
Indalloy 51[a]	862.8	63.3	27.0	578.0
Indalloy 51 + Cu	862.7	59.2	44.2	573.4
MgO + H_2O	861.7	63.7	7.7	588.2
MgO + H_2O + ethylene glycol	862.5	62.7	4.9	576.0
Silicone oil[b]	863.0	64.1	1.7	573.5
Sylguard 184[c]	864.5	56.1	9.8	578.1
Cellular silicone[d]	856.4	58.4	0.4	574.9

a. Indalloy 51 is a commercial eutectic alloy obtained from Indium Corporation of America.
b. The silicone oil is DC200-20 obtained from Dow Corning.
c. Sylguard 184 is a commercial silicone potting compound.
d. Cellular silicone is a solid polymer.

Table 2. Chemical Compositions of Materials Placed in Contact with Plutonium

Material	Composition (mass %)
Indalloy 51	62.5% Ga, 21.5% In, 16.0% Sn
Indalloy 51 + Cu powder	44.4% Indalloy 51, 55.6% Cu
MgO + H_2O	75% MgO, 25% H_2O (1.34:1 MgO:H_2O molar ratio)
MgO + H_2O + ethylene glycol	75% MgO, 25% solution containing 50% H_2O, 50% $C_2O_2H_6$ (2.8:1:0.32 MgO:H_2O: glycol molar ratio)
Silicone oil[a]	37.52% Si, 33.68% C, 20.30% O, 8.50% H
Sylguard 184	37.8% Si, 30.9% C, 23.9% O, 7.4% H
Cellular silicone	38% Si, 30% C, 25% O, 7% H[a]

a. The chemical composition of the silicone polymer is estimated.

Table 3. Initial and Final Gas-Phase Compositions Obtained from Mass Spectrometric Data

Test Material	Species	Initial %[a]	Final %
Indalloy 51	Ar	44.89	50.15
	N_2	43.56	48.70
	O_2	11.54	0.005
	CO_2	0.02	0.54
	HCl	--	0.17
	H_2	--	0.14
	H_2O	--	0.037
	CH_4	--	0.024
Indalloy 51 + Cu[b]	Ar	69.19	73.47
	N_2	24.36	25.67
	O_2	6.45	0.00
	CO_2	0.01	0.32
	H_2O	--	0.26
	HCl	--	0.17
	H_2	--	0.027
$MgO + H_2O$	Ar	44.97	50.98
	N_2	43.13	48.79
	O_2	11.90	0.005
	CO_2	0.02	0.003
	H_2	--	0.16
	CH_4	--	0.005
$MgO + H_2O$ + ethylene glycol	Ar	48.94	39.83
	N_2	40.38	32.82
	O_2	10.69	0.002
	CO_2	0.02	0.015
	H_2	--	26.77
	CH_4	--	0.47
	H_2O	--	0.016

Continued

Table 3. Initial and Final Gas-Phase Compositions Obtained from Mass Spectrometric Data (Continued)

Test Material	Species	Initial %[a]	Final %
Silicone oil	Ar	47.37	39.56
	N_2	41.62	34.70
	O_2	11.00	0.001
	CO_2	0.02	0.16
	H_2	--	23.96
	CH_4	--	1.50
	H_2O	--	0.015
Sylguard 184	Ar	42.75	40.70
	N_2	45.25	43.20
	O_2	12.00	0.002
	CO_2	0.02	0.26
	H_2	--	15.28
	CH_4	--	0.47
	H_2O	--	0.016
Cellular silicone	Ar	45.87	50.00
	N_2	42.80	46.60
	O_2	11.34	0.011
	CO_2	0.02	0.54
	H_2	--	2.24
	H_2O	--	0.23
	CH_4	--	0.052

a. Initial percentages are calculated values based on the final measured N_2:Ar ratios and the known molar of the constituents of air.

b. Original data for this sample showed a high O_2 percentage, indicating that air had leaked into the reactor shortly before the sample was analyzed. The reported final percentages are derived from those data, assuming that O_2 was depleted from the residual gas prior to the leak.

Relevant Reactions

Reactions occurring at the conditions of these tests include both radiolytic and chemical processes. Hydrogen is generated by radiolysis of hydrocarbons ($-CH_2$-containing substances) and other hydrogenous materials coexisting with plutonium or other sources of alpha radiation.

$$-CH_2- \text{ (s,l,g)} + \alpha\text{-particle} \rightarrow \text{C (s)} + H_2 \text{ (g)} . \quad (1)$$

Although the efficiency of a radiation-chemical effect is commonly indicated as a G value that defines the number of molecules destroyed or produced by each 100 eV of energy absorbed [4], measurement and use of the values is difficult, especially in heterogeneous systems. Most alpha particles produced by radioactive decay of plutonium in solids are self-absorbed. The fraction that escapes and contributes to radiolysis is strongly influenced by particle size or the specific surface area of the material. The use of areal rates is a tractable alternative to G values and facilitates extension of kinetic data to a range of material forms.

A sequence of chemical reactions involving oxygen, hydrogen, and water occurs at the conditions existing during these measurements. Water is an especially important species that exists either as a major constituent of the test material or at a concentration determined by the amount of moisture adsorbed on the internal surfaces of the reactor. Additional water may also form by the association of O_2 with H_2 generated by the radiolysis of hydrogenous materials or may be derived from other sources.

$$H_2 \text{ (ads)} + 1/2\ O_2 \text{ (ads)} \rightarrow H_2O \text{ (ads)} . \quad (2)$$

Although this reaction may occur in the gas phase, experiments indicate that the dominant process at 25°C involves the reaction of dissociatively adsorbed H_2 and O_2 on the surfaces of plutonium oxide and stainless steel [3]. Kinetic data for H_2O formation in a 2:1 H_2:O_2 2:1 mixture during exposure to outgassed PuO_2 show $dH_2O/dt = 1 \times 10^{-14}$ mol H_2O/cm^2 min. If the true surface area of oxide-coated plutonium metal is assumed to exceed the geometric value by a factor of 20, dH_2O/dt is about 2×10^{-13} mol H_2O/cm^2 min for metallic plutonium. The combination rate decreases by a factor of 30 as chemisorption of the water product blocks active surface sites on 15% of the oxide surface. Measurements involving exposure of H_2O to PuO_2 show that if radiolysis occurs, the rate is extremely slow, or the O_2 product is rapidly removed by Equation 2 or other chemical processes [3].

The Pu + H_2O reaction is relatively rapid in comparison with the reaction of metal with dry oxygen and proceeds with the formation of hydrogen as a gaseous product [5].

$$\text{Pu (s)} + 2\ H_2O \text{ (ads)} \rightarrow PuO_2 \text{ (s)} + 2\ H_2 \text{ (g)} . \quad (3)$$

In saturated water vapor (23.7 torr) at 25°C, dH_2/dt for the reaction of delta-phase plutonium, according to Equation 3, is 1×10^{-12} mol H_2/cm^2 min, a value derived by the extrapolation of

rates measured at high temperatures [6]. The rate is proportional to $(PH_2O)^{0.23}$ for water pressures in the 0.1 torr to 15 torr range [5].

The reaction of plutonium with dry air or oxygen is slow compared with oxidation via Equation 3 but is markedly enhanced by the presence of water [5]. In dry air, dO_2/dt for the alloy is on the order of 2×10^{-14} mol O_2/cm^2 min at 25°C [7]. In moist air, oxidation occurs at the rate determined by the partial pressure of water, but O_2 disappears from the gas phase, the H_2O concentration remains constant, and H_2 is not formed. This behavior is explained by occurrence of a water-catalyzed cycle in which metal reacts with H_2O at the rate of the Pu + H_2O reaction, but instead of associating as H_2, atomic hydrogen produced by the reaction combines with dissociatively adsorbed O_2 to re-form water.

$$Pu\ (s) + 2\ H_2O\ (ads) \rightarrow PuO_2\ (s) + 4\ H\ (ads)\ . \quad (4)$$

$$O_2\ (g) \rightarrow 2\ O\ (ads)\ . \quad (5)$$

$$\underline{4\ H\ (ads) + 2\ O\ (ads) \rightarrow 2\ H_2O\ (ads)\ .} \quad (6)$$

$$Pu\ (s) + O_2\ (g) \rightarrow PuO_2\ (s)\ . \quad (7)$$

In moisture-saturated air, $-dO_2/dt$ for the net reaction of delta-phase metal, according to Equation 7, is approximately 1×10^{-12} mol O_2/cm^2 min. As described by Equations 4–6, oxidation of plutonium in moist air proceeds by first consuming O_2 at the moisture-enhanced rate. After O_2 is depleted, H_2O reacts at the identical rate with the formation of H_2. This sequence precludes the coexistence of significant H_2 and O_2 concentrations during the reaction of moist air, but the formation of such mixtures is possible if hydrogenous material is present and the formation of H_2 via Equation 1 is faster than its consumption via Equations 2 and 7.

In the absence of oxygen and water, hydrogen formed by radiolytic and chemical reactions is expected to react with the metal to form plutonium hydride.

$$Pu\ (s) + H_2\ (g) \rightarrow PuH_2\ (s)\ . \quad (8)$$

Unlike oxidation, hydriding does not occur evenly over the entire metal surface but initiates at localized nucleation sites that increase in size over time until the entire surface is active [8]. Consequently, the reaction rate varies continuously with the degree of activation—from immeasurably small initial values to the maximum rate for a surface that is fully covered by hydride. The hydriding rate is proportional to the square root of the hydrogen pressure and is independent of temperature. The maximum value of $-dH_2/dt$ at 100 torr H_2 pressure is on the order of 1×10^{-2} mol H_2/cm^2 min. Hydriding apparently occurs only in the absence of significant O_2 or H_2O concentrations because those gases readily oxidize the hydride as it forms.

Hydride reactivity is demonstrated by the hydride-catalyzed reaction of O_2 and N_2 with the plutonium metal [9]. Hydride-coated metal reacts violently with O_2 ($-dO_2/dt = 3 \times 10^{-2}$ mol

O_2/cm^2 min at the 160 torr pressure of O_2 in air) and at a surprisingly rapid rate with air through a process that indiscriminately consumes both nitrogen and oxygen. The reaction of PuH_2 with O_2 and N_2 in air produces hydrogen that is not released as H_2, but moves into the metal and continually re-forms hydride ahead of the advancing reaction of air. The net process is most easily described by separate equations leading to the formation of dioxide (Equation 7) and mononitride.

$$Pu\ (s) + 1/2\ N_2\ (g) \rightarrow PuN\ (s)\ . \qquad (9)$$

At one atmosphere pressure, air is consumed at a temperature-independent rate of 2×10^{-3} moles/cm^2 min. Rapid formation of nitride is apparently promoted by heating from the oxidation reaction, but the hydride-catalyzed reaction of N_2 at room temperature may occur independent of oxidation.

The chloride-catalyzed reaction of plutonium with water is a process that occurs in salt water [10,11] and has recently been identified as the likely source of rapid corrosion in glovebox lines containing trace levels of gaseous hydrogen chloride [12]. Corrosion of the metal by HCl forms $PuCl_3$ on the surface. Absorption of moisture from the glovebox atmosphere by the deliquescent product forms a concentrated chloride solution and catalyzes the reaction of plutonium with water to form the plutonium monoxide monohydride and hydrogen.

$$Pu\ (s) + H_2O\ (soln) \rightarrow PuOH\ (s) + 1/2\ H_2\ (g)\ . \qquad (10)$$

Kinetic data are not available, but a reaction rate can be estimated from the observed formation of a thick product layer on the metal during overnight exposure to an argon atmosphere containing moisture and less than 10 ppm HCl (g). Formation of a 1 μm-thick layer of black PuOH (theoretical density = 10.80 g/cm^3) over a 15-hour period corresponds to an average dH_2/dt of 2×10^{-9} mol H_2/cm^2 min for Equation 10.

Relevance of the preceding discussion to experimental observations in this study is shown by the consideration of thermodynamic and kinetic factors. Mobile species (O_2, H_2, H_2O, and N_2) in the test systems attempt to reach thermodynamic equilibrium with plutonium metal by forming oxide, hydride, and nitride. Reactions of plutonium with other elements such as carbon, silicon, and gallium are also favorable. However, the transport processes required for their reactions with the metal are very slow at 25°C, and significant interaction is considered unlikely, especially when the metal is covered with a coherent layer of oxide. The course of reaction between plutonium and the test materials is determined by kinetics; the most rapid reaction occurs at each point in time and the products are not necessarily in the most stable chemical state.

In Table 4, a summary of the kinetic data for possible reactions shows that reaction rates of potential processes differ by as much as 10^{12}. Two distinct groups of rate behavior are seen: (1) hydriding and hydride-catalyzed reactions are the most rapid and (2) reactions involving water and oxygen are slower by factors of 10^6 to 10^{11}. Hydride formation and subsequent hydride-catalyzed oxidation of the metal by O_2 might be expected, but immediate occurrence of those reactions is unlikely because H_2 is not initially present in the test systems. Although sufficient H_2 might be produced by the rapid radiolysis of hydrogenous material, the formation of hydride is precluded by the presence of oxygen. The most rapid reaction (hydride-catalyzed oxidation of plutonium) involves oxidation of PuH_2 by O_2 at an extremely rapid rate for a gas-solid reaction. Therefore, the formation of hydride is not anticipated as long as oxygen is present. Hydriding in the presence of H_2O vapor is not expected because H_2 is a product of the Pu + H_2O reaction. Since water is present in some test materials and adsorbed on all surfaces in the reactor, occurrence of the water-catalyzed Pu + O_2 and the Pu + H_2O reactions is expected initially.

Determination of the reactions responsible for observed pressure changes relies on the correlation of observed and known kinetic behavior. The sign of the pressure change and the magnitude of the reaction rate provide reliable criteria for identifying specific chemical reactions.

Table 4. Summary of Kinetic Data for Reactions of Delta-Phase Plutonium at 25°C

Reaction	Conditions	Rate (mol/cm^2 min)	Ref.
PuH_2-catalyzed Pu + O_2	100 torr O_2	$-dO_2/dt = 3x10^{-2}$	9
Pu + H_2	100 torr H_2	$-dH_2/dt = 1x10^{-2}$	8
PuH_2-catalyzed Pu + air	760 torr air	$-dN_2 + O_2/dt = 2x10^{-3}$	9
Cl^--catalyzed Pu + H_2O	<10 ppm HCl, low humidity	$dH_2/dt = 2x10^{-9}$	12
H_2O-Catalyzed Pu + O_2	satd.H_2O vapor, 760 torr air	$-dO_2/dt = 1x10^{-12}$	5
Pu + H_2O	saturated H_2O vapor	$-dO_2/dt = 1x10^{-12}$	5,6
H_2 + O_2	2:1 molar ratio, 125 torr	$dH_2O/dt = 1x10^{-13}$	3
Pu + O_2	760 torr dry air	$-dO_2/dt = 2x10^{-14}$	5,7

Results and Discussion

Pressure changes derived from P-t data are presented as a function of elapsed time in Table 5 and in Figures 1, 2, and 3. Compositions of the residual gases at the termination of the measurements are listed in Table 3. These data imply that the behavior of the test materials is divergent and dependent on chemical and physical properties. Net pressure decreases consistent with the complete reaction of O_2 are observed for metallic and inorganic materials. Both increases and decreases in the net pressure are observed for materials containing hydrogenous constituents. However, similarities appear in the depletion of O_2 from all residual gas mixtures and in the appearance of highly fluctuant pressure behavior during the first 0.5 year of the tests.

Table 5. Measured Pressure Changes in Test Reactors as a Function of Time[a]

Elapsed Time (years)	Indalloy 51	Indalloy 51 + Cu	MgO + H_2O	MgO + H_2O + Glycol	Silicone Oil	Sylguard 184	Cellular Silicone
0.019	--	--	–11	1	11	8	13
0.027	--	--	–17	–5	10	7	11
0.041	–13	–11	–18	–8	11	7	11
0.093	--	--	–25	–24	6	2	6
0.134	–14	–10	–20	–34	4	–3	2
0.186	--	--	–18	–32	2	–7	–2
0.258	–14	–9	–24	–18	2	–2	–2
0.296	--	--	–22	–9	6	5	6
0.359	–14	–6	--	--	10	7	5
0.457	--	--	--	--	12	3	1
0.608	–14	–10	–17	–3	14	–14	–12
2.22	–32	–21	11	23	35	–24	–22
3.27	–35	--	–7	36	--	–31	–28

a. Measured pressure is reported in torr and is corrected for calibration errors by using a multiplication factor of 1.76.

The results of each test are evaluated individually in an effort to address unique behavior. Descriptions of the initial specimens and the final products of the tests are supplemented by color photographs presented in the appendices. An important feature of the test configuration is the constraint placed on each system if O_2 reacts and N_2 does not. In that case, the pressure

cannot drop below that resulting from the consumption of O_2. The minimum pressure is not altered by transient formation and reaction of H_2, but the presence of residual H_2 must be considered in determining the ultimate minimum value.

The presentation order of the test results is selected to facilitate their interpretation. Although simple and readily defined behavior was anticipated for liquid alloys, interpretation of the results for those tests was surprisingly difficult and is presented last. The assessments of the results for the tests with MgO are presented first because their interpretation is simplified by the known presence of H_2O in the slurries and the availability of reliable kinetic data for reactions involving water.

MgO + H_2O + Ethylene Glycol

Visual inspection of the products indicates that material transport, polymerization, and radiolysis of ethylene glycol occurred during the 3.3-yr test. As shown in the photographs (Appendix A), the initial plutonium specimen had the characteristic appearance of delta-phase metal covered by a silver-gray oxide layer formed during processing. The MgO slurry initially covered a 15 cm^2 area of the cup, but its size was markedly reduced after the test. All surfaces in the reactor were covered with a thin, rust-brown, refringent layer with a varnish-like appearance. Thick deposits of the layer that formed on the reactor lid directly above the slurry were readily removed by scraping them with a spatula. Shrinkage of the slurry and deposition of the layer are consistent with vapor-phase migration of the glycol and polymerization via a reaction involving the double bond of ethylene glycol. The prominent rust color on the contact surface of the test residue is attributed to the formation of carbon-rich products by the radiolytic degradation of glycol.

Corrosion of the plutonium is evident on all surfaces of the metal specimen, but appears most extensive on the bottom surface away from the test material. Although enhanced reactivity of the convex surface might result from fracture of the protective oxide layer caused by tensile stress during the pressing of the cup, that possibility seems unlikely because bottom surfaces inside and outside the deformation zone appear equally corroded. A photograph of the convex surface (Appendix A) shows a residual region of gray color that was present on the entire surface upon the opening of the reactor. After exposure to air, that surface changed to a color consistent with the presence of khaki-colored plutonium dioxide beneath a rust-brown film of partially radiolyzed glycol.

Quantitative results suggest the occurrence of three major processes during the course of the test. P-t data (Figure 1) show that a small (1 torr) initial pressure increase is followed by a steep pressure decrease, an equally steep pressure increase, and a progressive pressure

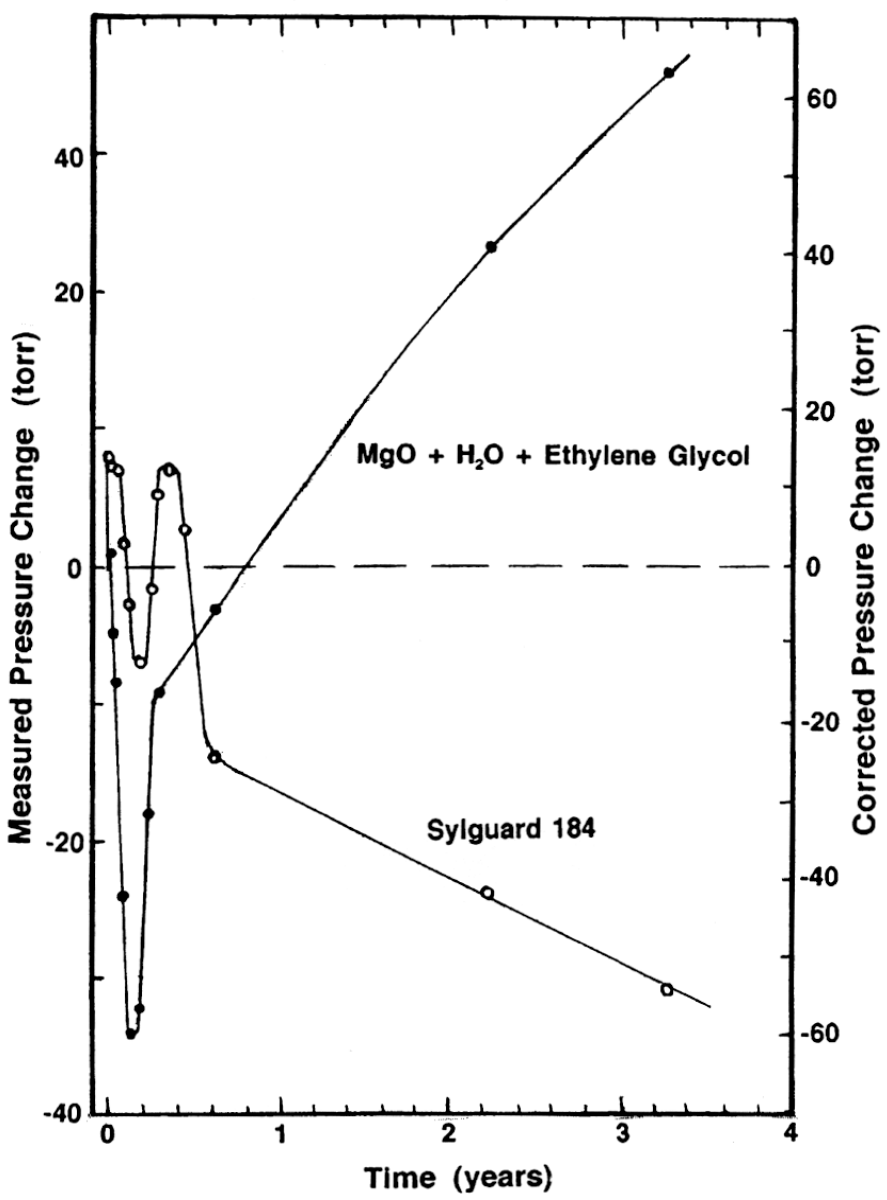

Figure 1. Time dependence of pressure during the tests with the $MgO + H_2O$ plus ethylene glycol slurry and with Sylguard 184.

increase beyond 0.3 years. MS results in Table 3 show that O_2 and H_2O were depleted and that H_2 accumulated during the test. The initial and long-term pressure increases are attributed to the formation of H_2 by the radiolysis of glycol. The value of dH_2/dt derived from P-t data for the 0.3–0.6-yr period is 7.0×10^{-11} mol H_2/cm^2 min, assuming that the entire 80 cm^2 plutonium surface was covered by glycol. On the basis of the data in Table 4, the rates of

5.9×10^{-10} and 3.8×10^{-10} moles/cm^2 min derived from P-t data for the sharp decrease and increase in pressure are assigned to $-dO_2/dt$ and dH_2/dt for the water-catalyzed Pu + O_2 and the Pu + H_2O reactions, respectively. As expected, these reactions occur in sequence and are the only processes that can account for the depletion of O_2 and H_2O at equal rates. Comparison of the measured rates with the anticipated values in Table 4 show that the reactions are substantially more rapid than predicted by the extrapolation of high-temperature data to 25°C.

The observed extent of the reaction is consistent with the consumption of O_2 and H_2O and the accumulation of H_2. The measured mass loss (0.4 g) by the plutonium specimen plus the estimated amount (0.4 g) of oxide product remaining on the plutonium surface after the test are in good agreement with the theoretical extent (1.0 g) of plutonium oxidation by O_2 and H_2O. The amount of oxide remaining on the metal surface was estimated by using the 4–5-µm-thick oxide layer predicted from a correlation of thickness with reaction temperature [13]. The amount of H_2O (2.0×10^{-3} mol) reacting during the test was calculated from the pressure increase measured during the 0.2–0.3-yr period in Figure 1. The agreement of calculated and observed extents of reaction supports the conclusion that metal was not consumed by the Pu + H_2 reaction during the test. The color change observed upon exposure of the metal to air most likely results from oxidation of substoichiometric oxide to PuO_2.

Information on the chemical behavior of the magnesium oxide slurry is derived from the experimental results. The slurry hardens and shrinks as dihydroxide is formed by hydration of MgO.

$$MgO\ (s) + H_2O\ (l) \rightarrow Mg(OH)_2\ (s)\ . \qquad (11)$$

The rate of this reaction is relatively slow because the slurry could be prepared and handled for a period of time without hardening. However, the amount of water that reacted with the plutonium was only 6% of that present in the slurry, suggesting that Equation 11 was essentially complete before O_2 was consumed and the Pu + H_2O reaction initiated. The absence of free water is consistent with the 2.8:1 molar ratio of MgO:H_2O in the slurry; a mixture containing only 35% of the water required for complete hydration of the magnesium oxide. As shown by data in Table 3, the formation of magnesium carbonate by the reaction of carbon dioxide with $Mg(OH)_2$ is suggested by the low CO_2 concentrations in the residual gases present in this test and in the companion test with the MgO + H_2O slurry. The CO_2 concentrations observed in other tests are noticeably larger. Radiolysis of water that is chemisorbed as hydroxide in $Mg(OH)_2$ is possible, but is not indicated by the MS results.

$MgO + H_2O$

The examination of solid residues from the test shows products similar to those obtained from the glycol-containing slurry. However, as shown by the photographs (Appendix B), shrinkage of the hardened test material appeared to be less than for the glycol-containing slurry, and coating of the surfaces by polymeric product was not observed. Corrosion of the metal is evident and most extensive on the convex surface of the specimen. Dark gray areas on that side of the sample suggest localized regions with different chemical behavior. Corrosion pits characteristic of hydriding are seen on the upper surfaces around the cup.

The P-t data for the $MgO + H_2O$ test material in Figure 2 show initial behavior similar to that for $MgO + H_2O$ + ethylene glycol. As indicated by rates of 5.2×10^{-10} moles/cm^2 min for the pressure decrease and 2.3×10^{-10} moles/cm^2 min, the initial part of the pressure increase, the water-catalyzed $Pu + O_2$ and the $Pu + H_2O$ reactions occurred in sequence as expected. However, further kinetic evaluation is not possible because of an apparent failure of the pressure transducer. MS data for the residual gas show no H_2O, a trace of O_2, and a low H_2 concentration. After the transducer failed, the pressure in the reactor apparently increased as H_2 formed via the $Pu + H_2O$ reaction and then decreased as the H_2 was consumed by the $Pu + H_2$ reaction. The relatively large mass loss (1.9 g) of the plutonium specimen, compared with that observed for the glycol-containing MgO slurry, is consistent with the presence of more water (75% of that required for the complete hydration of MgO) and its reaction to form additional PuO_2 and PuH_2.

The combined results of the tests with MgO slurries define the sequence of reactions occurring in systems containing oxygen and water. The water-catalyzed $Pu + O_2$ and the $Pu + H_2O$ reaction result in a characteristic P-t pattern of a pressure decrease from O_2 consumption followed by an equally rapid increase from H_2 generation. For the quantities of O_2 and H_2O present in the tests, these reactions are complete after approximately 0.3 yr. Hydrogen produced by the $Pu + H_2O$ either reacts with metal to form hydride or accumulates in the system.

Silicone Oil

Residues from the test with silicone oil show evidence of extensive radiolysis. As seen in photographs (Appendix C), the plutonium specimen was covered by oil that had spilled during handling of the reactor and had polymerized as a layer of varnish-like product. Residual fluid in the cup was dark brown and sufficiently viscous that it would not flow. Areas in which the varnish layer had been removed by spallation of the corrosion product existed on the convex surface. Additional corrosion of the metal apparently occurred under the polymer layer.

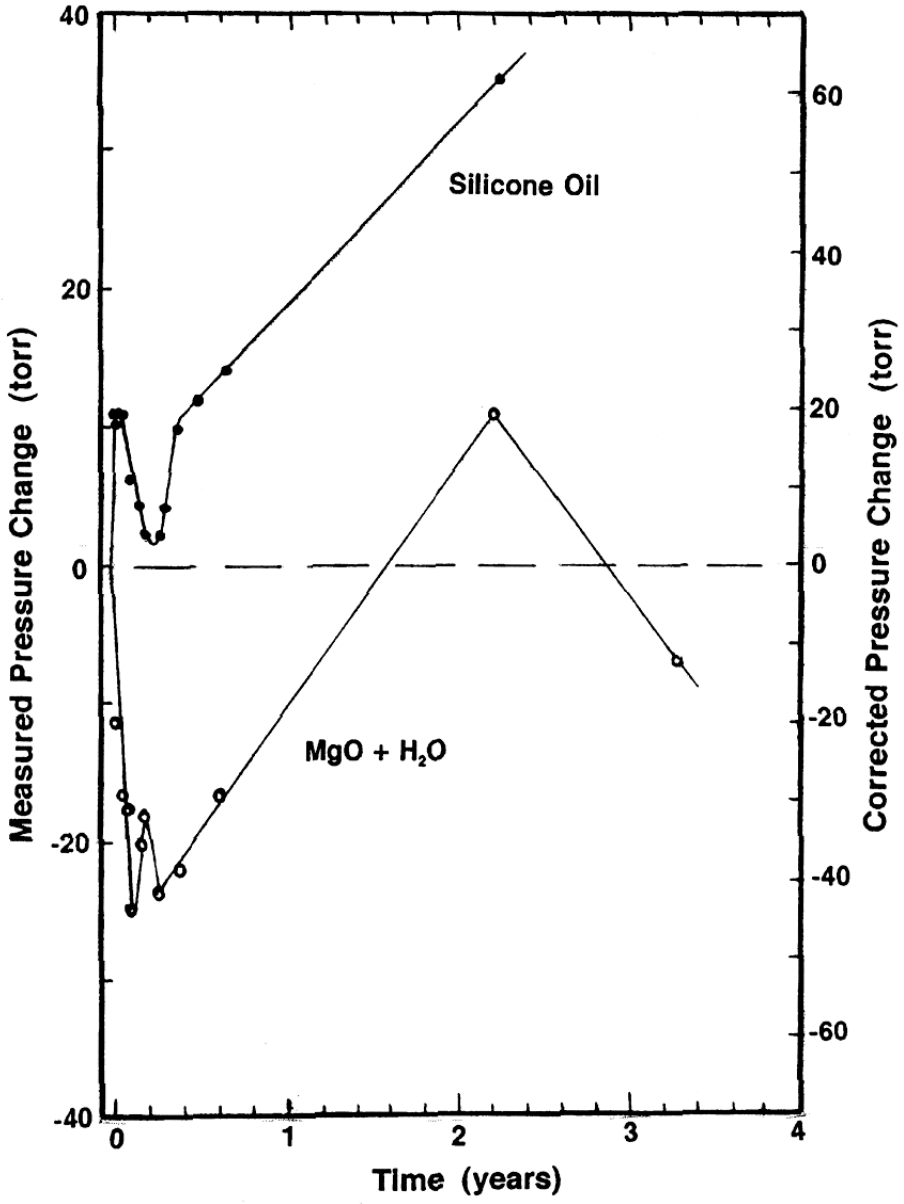

Figure 2. Time dependence of pressure during the tests with the $MgO + H_2O$ slurry and with silicon oil.

During the final measurements, the internal pressure was at ambient, and an inspection of the reactor showed that the valve was not tightly closed.

P-t data in Figure 2 show a pattern consistent with rapid initial H_2 generation by the radiolysis of hydrogenous material, reaction of O_2 by the water-catalyzed process, formation of H_2 by the $Pu + H_2O$ reaction at an equally rapid rate, and radiolytic generation of H_2 at a constant rate beyond 0.3 yr. Respective rates derived for these steps are

$dH_2/dt = 1.1 \times 10^{-9}$ mol H_2/cm^2 min, $-dO_2/dt = 1.2 \times 10^{-10}$ mol O_2/cm^2 min, $dH_2/dt = 1.5 \times 10^{-10}$ mol H_2/cm^2 min, and $dH_2/dt = 2.6 \times 10^{-11}$ mol H_2/cm^2 min. The rates for the O_2 and H_2O reactions are a factor of 4 less than observed for aqueous MgO slurries and are consistent with the presence of lower water concentrations in this test. MS data obtained for the residual gas show only a trace of O_2, indicating that gases escaped from the reactor through the valve, but that air did not enter. The presence of a high H_2 concentration (24%) is consistent with continuous accumulation of radiolytic hydrogen during the test. Although corrosion of the metal and spallation of product were visibly evident, the mass of the plutonium specimen increased by 0.9 g because of the polymerized oil layer on the surface.

Cellular Silicone

An inspection of the products present after the termination of the cellular silicone test shows evidence of radiolysis and corrosion. Evidence for the spread of hydrogenous material is not seen in product photographs (Appendix D), and the radiolytic reaction was apparently confined to the 12 cm^2 area of the silicone polymer. Brown discoloration of the test material was extensive at the contact surface, and embrittlement was indicated by fracture of the sample when it was flexed. The convex surface was initially gray but turned to the yellow-green to khaki color of PuO_2 after exposure to air. Silver-gray areas that remained on that surface are apparently unspalled regions of the original oxide layer on the alloy. Photographs taken of the upper plutonium surface immediately after opening the reactor show localized black pits characteristic of hydriding.

The evaluation of P-t data in Figure 3 and the MS results in Table 3 are consistent with a reaction sequence involving initial H_2 generation by the radiolysis of the silicone, reaction of O_2 by the water-catalyzed process, formation of H_2 by the $Pu + H_2O$ reaction, and concurrent generation and consumption of H_2 by radiolysis and hydride formation. Respective rates derived for these steps are $dH_2/dt = 8.8 \times 10^{-9}$ mol H_2/cm^2 min, $-dO_2/dt = 1.7 \times 10^{-10}$ mol O_2/cm^2 min, $dH_2/dt = 4.1 \times 10^{-10}$ mol H_2/cm^2 min, and $-dH_2/dt = 2.2 \times 10^{-11}$ mol H_2/cm^2 min. The first three rates are remarkably consistent with those for silicone oil. The final rate is the average net value resulting from simultaneous formation of H_2 by radiolysis and consumption by a more rapid $Pu + H_2$ reaction.

The preceding interpretation of kinetic behavior is consistent with the measured changes in the sample mass and with the final pressure expected for the reaction of O_2. The sum of the observed mass loss (0.6 g) by the plutonium specimen and the calculated mass (0.4 g) of the adherent product is in good agreement with the extent (1.4 g) estimated for oxidation and

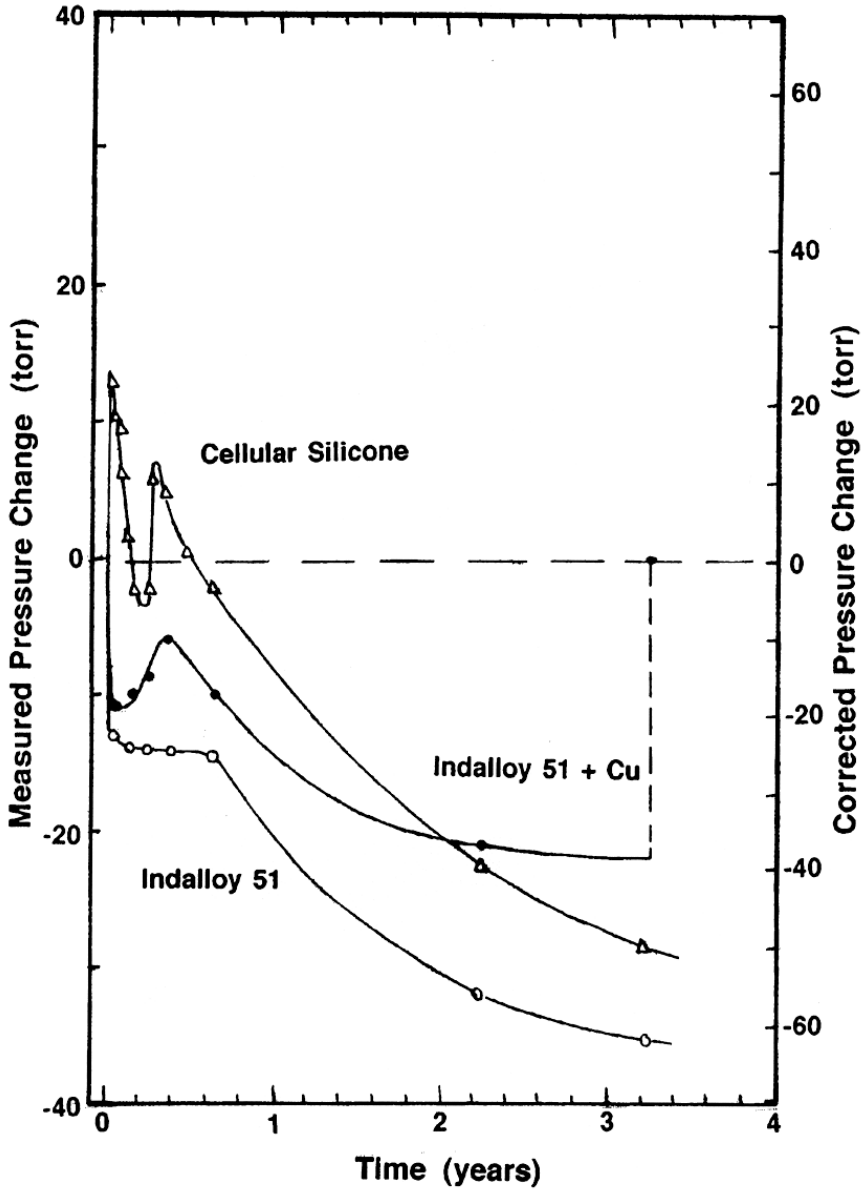

Figure 3. Time dependence of pressure during the tests with Indalloy 51, with Indalloy 51 plus copper powder, and with cellular silicone.

hydriding. If the residual H_2 (12 torr) had reacted, the total pressure decrease would have been 62 torr, a value in close agreement with the theoretical change expected for the reaction of O_2 at an initial partial pressure of 65 torr.

Sylguard 184

Products of the test with a binary silicone potting compound also show evidence of radiolysis and plutonium corrosion. Unlike other fluid materials, this compound remained in place and cured as a clear silicone polymer that covered 20 cm^2 of the plutonium surface. As seen in the photographs (Appendix E), radiolysis is indicated by discoloration at the compound-metal interface. As in other tests, corrosion is most extensive on the convex metal surface, but the product had a distinctive, medium-brown color characteristic of PuN on 10 cm^2 of that surface. Hydriding is suggested by localized pitting of the upper surface near the test material. The irradiated polymer adhered strongly to the metal and exhibited tough rubber-like properties during attempts to remove it from the metal surface.

P-t data for the silicone polymer in Figure 1 suggest that five distinct sequential processes occurred during the test. In the order of occurrence they were: (1) the linear segments of the curve corresponding to the formation of H_2 by the radiolysis of hydrogenous material, (2) the water-catalyzed oxidation of plutonium by O_2, (3) the H_2 generation by the Pu + H_2O reaction, (4) the consumption of H_2 by the Pu + H_2 reaction, and (5) a process involving simultaneous formation of H_2 by radiolysis and PuN by the hydride-catalyzed Pu + N_2 reaction. The respective rates measured for the first four reactions are $dH_2/dt = 4.1 \times 10^{-9}$ mol H_2/cm^2 min, using a 20 cm^2 area; $-dO_2/dt = 2.3 \times 10^{-10}$ mol O_2/cm^2 min, using a 60 cm^2 area; $dH_2/dt = 2.1 \times 10^{-10}$ mol H_2/cm^2 min, using a 60 cm^2 area; and $-dH_2/dt = 1.3 \times 10^{-9}$ mol H_2/cm^2 min, using an active area of 10 cm^2. The measured net rate during the final process is -1.0×10^{-10} mol/cm^2 min.

P-t and MS results are consistent with the formation of PuN by the hydride-catalyzed Pu + N_2 reaction. Accumulation of a high H_2 concentration (15.3% or 80 torr partial pressure) suggests that hydriding ceased when nitriding apparently initiated after 0.6 yr into the test. If the accumulated H_2 had reacted, the total pressure decrease would have been 167 torr, a value that far exceeds the theoretical decrease expected for reaction of O_2 at an initial partial pressure of 87 torr. A reaction of N_2 is the only process that can account for this additional pressure decrease. Generation of the accumulated H_2 at 20 cm^2 contact area during the time period of the final step corresponds to $dH_2/dt = 2.6 \times 10^{-10}$ mol H_2/cm^2 min. In order to give the observed net rate of the reaction,$-dN_2/dt$ must equal 3.6×10^{-10} mol H_2/cm^2 min. The validity of this interpretation is assessed by comparing the observed and theoretical amounts of plutonium corrosion. The observed extent of plutonium consumption (3.8 g) includes the measured mass loss (3.4 g) and the estimated amount (0.4 g) of adherent product remaining on the specimen. Use of the derived reaction rate for the Pu + N_2 reaction predicts that 2.41 g of plutonium reacted during the final 2.6 yr of the test. A combination of the amount of metal

involved in nitriding with the amounts consumed by the reaction of O_2 (0.77 g), H_2O (0.27 g), and H_2 (0.41 g) yields a theoretical extent of corrosion (3.86 g) that is in excellent agreement with the observation.

Indalloy 51

Examinations of products formed during the exposure of delta-phase plutonium alloy to the liquid alloy are surprising. As shown by the photographs (Appendix F), most of the alloy was lost from the plutonium cup during the course of the test and had coalesced in the reactor or adhered to the stainless steel specimen stand. However, two pieces of solidified alloy residue remained in the cup and were bound to the plutonium surface. Small irregular regions of silver on the convex surface of the plutonium specimen were easily removed and appear to be residual regions of the original oxide layer, not adherent alloy. Careful inspection shows that these silver areas reside on top of a black product layer, which in turn covers the greenish-yellow to khaki layer characteristic of PuO_2. Similar, but less clearly defined, product layers are seen on the concave plutonium surface.

The P-t behavior in Figure 3 is especially surprising. The onset of water-catalyzed oxidation is indicated by an initial pressure decrease with $-dO_2/dt = 6.1 \times 10^{-10}$ mol O_2/cm^2 min. This reaction involved water that was apparently present as H_2O adsorbed on reactor surfaces. However, after 0.1 year, the pressure abruptly became constant, implying that the reaction had stopped. After 0.7 yr, reaction resumed at a significantly slower rate, and the total decrease in pressure (63 torr) gradually approached that of the initial O_2 partial pressure (66 torr).

A consistent interpretation of this perplexing P-t behavior is suggested by MS results (Table 3) showing that a large concentration (1700 ppm) of HCl was present in the residual gas at the termination of the experiment. Hydrogen chloride was observed in both tests involving Indalloy 51 but did not appear in any of the other systems, suggesting that the alloy was contaminated with trace amounts of metal chlorides ($GaCl_3$, $InCl_3$, $SnCl_2$) typically used in the purification of the constituent metals in Indalloy 51. When exposed to moisture, these chlorides hydrolyze to form hydroxides and HCl. After sufficient HCl had formed, its reaction with plutonium produced $PuCl_3$ on the metal surface. Adsorption of water by the deliquescent chloride resulted in the chloride-catalyzed $Pu + H_2O$ reaction described by Equation 10. Fortuitously, the rate of H_2 formation equaled that of the water-catalyzed $Pu + O_2$ reaction and resulted in a constant P-t curve. Therefore, $dH_2/dt = 6 \times 10^{-10}$ mol H_2/cm^2 min and the PuOH formation rate is 1.2×10^{-9} mol/cm^2 min, values that are in remarkably close agreement with the estimated rate in Table 4. Formation of PuOH accounts for appearance of the black layer

on the metal surface. Reduction of the H_2O concentration by this reaction resulted in the consumption of the remaining O_2 at a relatively slow rate ($-dO_2/dt = 1.0 \times 10^{-11}$ mol O_2/cm^2 min). As indicated by a low residual hydrogen concentration, H_2 formed by the chloride-catalyzed reaction of water also reacted to form hydride. The measured mass loss of 1.6 g by the plutonium specimen is consistent with the consumption of 1.5 g of metal by O_2, H_2O, and H_2 during the test with Sylguard 184, but a quantitative assessment is not possible for this test.

The formation of a solid product bound to the plutonium surface suggests that Indalloy 51 reacted with the plutonium metal during extended contact at room temperature. Although stable binary compounds of plutonium with gallium, indium, and tin are known, their formation in the test configuration was not anticipated because the oxide layer on metal usually acts as a kinetic barrier to such interactions. However, a reaction between plutonium and gallium, the lowest-melting and most mobile alloy constituent, is the most reasonable explanation for the observed behavior. That process may have been promoted by the action of metal chlorides and HCl in degrading the integrity of the oxide layer beneath the test specimen. A reaction of gallium with plutonium is expected to form intermetallic compounds at the oxide-metal interface and to leave a gallium-depleted solid residue of indium and tin on the surface.

XRD for the metal surface (sample ID No. BM 88175) near the reaction zone shows the presence of PuO_2 and Pu_2OC (reported as PuO) with measured lattice parameters of 5.355 Å and 4.973 Å, respectively, plus weak reflections of the underlying delta-phase metal. Diffraction data are not reported for the solid surface product (Appendix F) formed, and it is uncertain whether that material was amorphous or was not analyzed.

SEM, backscattered secondary electron (BSE) and x-ray fluorescence (microprobe) images of the metallographically sectioned plutonium specimen (sample ID No. BM 88175) show that a layer (>90 µm thickness) of gallium-rich alloy formed at the surface during the test. Elemental compositions determined from the data show a large gradient across the reaction product. Molar ratios derived from these data are presented in Table 6 as a function of distance from the product-plutonium interface. As expected, the plutonium content is highest near the interface and decreases with distance from the interface. Results show that the gallium content increases sharply relative to the plutonium over the first 10 µm of the product layer and then increases at a slower rate. Compositions range from values corresponding to gallium-saturated delta-phase alloy near the interface to values approaching $GaPu_4$ at distances greater

Table 6. Compositions of the Plutonium-Indalloy 51 Product as a Function of Distance from the Reaction Interface

Distance from the Pu-Product Interface (μm)	Molar Ratio			Anticipated Compounds[b]
	Pu	Ga	In[a]	
2	1	0.1	0.00	δ-phase Pu + Pu_3Ga
5	1	1.6	0.02	PuGa + $PuGa_2$
7	1	2.6	0.04	$PuGa_2$ + $PuGa_3$
15–40	1	3.0	0.17	$PuGa_2$ + $PuGa_3$
40–55	1	3.4	0.20	$PuGa_3$ + $PuGa_4$

a. Results for indium are based on median values of the fluctuating concentration.
b. Anticipated compounds are those expected on the basis of the measured composition and known phase equilibria of the plutonium-gallium system. Their presence has not been verified experimentally.

than 40 μm from the interface. The indium concentration in the product is very low at the interface, increases with distance from the interface, and exhibits noticeable fluctuations (between 3 and 9 mass%) at distances greater than 15 μm from the interface into the product. The tin concentration is very low across the product layer but also increases progressively with distance from the interface and approaches 0.5 mass% at a distance of 50 μm from the product-plutonium interface.

The composition profile across the product implies that the reaction occurred by the diffusion of constituent metals from the Indalloy 51 alloy into a stationary plutonium phase at room temperature. If plutonium were mobile, the molar ratio of Ga:In:Sn in the product should correspond to that of the liquid alloy (6.6Ga:1.4In:1Sn). The ratio of the metals (198Ga:10In:1Sn) observed in the product at a distance of 50 μm from the reaction interface is consistent with differences in mobility indicated by the melting points of gallium, indium, and tin (30, 156, and 232°C, respectively). Gallium should have the highest mobility and, as expected, is the only element coexisting with plutonium at the reaction interface. Tin is expected to be least mobile and appears only at low levels in the plutonium-containing product. By inference, the solid product remaining on the specimen surface is a solid residue enriched in tin and indium.

Indalloy 51 + Cu

Products formed during the test with a mixture of Indalloy 51 and copper powder are similar to those from the test with Indalloy 51. However, as shown by the photographs (Appendix G), the alloy-copper mixture solidified without loss of material from the cup and appeared to involve the crystallization of a copper-containing intermetallic compound as large silver needles in the product. The upper surface of the solid alloy is covered by a porous, gray layer that may have resulted from hydrolysis of chloride impurities. The corrosion product on the convex surface of the plutonium specimen shows the presence of three product layers. Large fractions of the surface were covered by the original silver layer on the metal and by khaki-colored oxide. Careful inspection shows that a third layer of black product existed between these layers. The solidified alloy adhered to the plutonium specimen, and its removal resulted in the transfer of oxide to the alloy and the retention of alloy on the plutonium surface. Test material remained on the plutonium surface at several locations, suggesting that a chemical interaction of the alloy with plutonium may have occurred to a limited extent.

The possibility of air leakage into the reactor was suggested by the discovery of a loose tube fitting on the reactor assembly during preparation for gas sampling. MS results verified that a high O_2 concentration was present. A small amount of H_2 remained in the mixture, suggesting that a leak most likely occurred during handling shortly before sampling. The initial gas composition in Table 3 was calculated assuming that O_2 from the initial fill had been completely consumed prior to the leak and that the ratio of constituents in the additional gas were equal to values for air.

The P-t results in Figure 3 are similar to those for Indalloy 51. MS data show the presence of HCl (2600 ppm) in the residual gas. A modest pressure rise occurred during the time period of constant pressure in the companion test with liquid alloy. An entirely consistent evaluation is achieved by a parallel interpretation of the results. The water-catalyzed Pu + O_2 proceeds at a characteristic rate ($-dO_2/dt = 5.2 \times 10^{-10}$ mol O_2/cm^2 min) until formation and hydration of $PuCl_3$ results in the onset of the chloride-catalyzed Pu + H_2O reaction. A modest pressure rise (6×10^{-11} mol/cm^2 min) shows that the rate of H_2 formation exceeds the rate of O_2 consumption and yields net rates of $dH_2/dt = 6 \times 10^{-10}$ mol H_2/cm^2 min and dPuOH/dt = 1.2×10^{-9} mol PuOH/cm^2 min for the chloride-catalyzed Pu + H_2O reaction. Thereafter, residual O_2 reacts at a relatively slow rate ($-dO_2/dt = 1.5 \times 10^{-11}$ mol O_2/cm^2 min) in the low humidity atmosphere, and H_2 is consumed by hydride formation. The observed mass loss (0.9 g) by the plutonium specimen is consistent with the relatively low O_2 concentration (6.45%, 37 torr partial pressure) in the initial gas mixture.

Conclusions

Kinetic results for the chemical and radiolytic reactions observed in this study are consistent with earlier work, define experimental rates more accurately, and provide data for reactions that have been described previously. The sequential occurrence of water-catalyzed Pu + H_2O and the Pu + H_2O reactions in systems containing moist air is demonstrated by the initial consumption of O_2 at a rate that is consistently equal to that for the subsequent formation of H_2. Measured $-dO_2/dt$ and dH_2/dt results obtained for these reactions in tests with liquid metals and aqueous slurries yield an average rate of $5 \pm 1 \times 10^{-10}$ mol/cm^2 min, a value that exceeds the extrapolated rate at 25°C by a factor of 500. Equal rates for the two reactions are also observed in systems containing silicones, but the average rate in those systems is $2 \pm 1 \times 10^{-10}$ mol/cm^2 min. These results suggest that the corrosion rate of delta-phase plutonium is markedly enhanced by moisture at room temperature.

Results from liquid alloy systems provide the first-rate data for the chloride-catalyzed reaction of plutonium with water vapor in the presence of HCl. At 25°C, dH_2/dt obtained for the reaction is 6×10^{-10} mol H_2/cm^2 min. This value is in excellent agreement with the qualitative prediction in Table 4 but is substantially less than the rates (1×10^{-7}–1×10^{-6} mol H_2/cm^2 min) observed for the chloride-catalyzed reaction in the 1 M aqueous chloride solutions [10]. The results suggest a strong dependence of the corrosion rate on water concentration and demonstrate that the chloride-catalyzed process is faster than the water-catalyzed Pu + O_2 reaction, with the ability to slow the oxidation rate by extracting water from the chemical system. The occurrence of the chloride-catalyzed reaction depends on a source for HCl and is to be anticipated only in systems where that potential exists. A somewhat surprising conclusion reached in this study is that molecular (nonionic) chlorides of certain metals are potential sources of HCl when exposed to moisture. The formation of HCl in dry inert atmospheres was not anticipated.

The observed reaction of gallium with plutonium at room temperature shows that gallium penetrates the oxide barrier in the plutonium surface and diffuses into plutonium at a significant rate. The total migration distance approached or exceeded 0.1 mm during the 4-yr period between the initiation of the test and the analysis of the specimen, but the total distance between the reaction front and the PuO_2 layer marking the initial interface was not determined. However, the measured composition profile should be adequate for estimating the diffusion coefficient of gallium in plutonium.

Measurements of areal rates for the radiolytic generation of H_2 by silicones and ethylene glycol in contact with weapons-grade plutonium metal provide practical data for estimating the extent of hydrogen production by organic materials over time. Relatively rapid rates

($dH_2/dt = 4 \pm 3 \times 10^{-9}$ mol H_2/cm^2 min) are observed immediately after hydrogenous material and plutonium are placed in contact, but "burn-out" of hydrogen at the plutonium interface results in substantially slower rates over time. After 0.3–0.4 yr, observed rates ($dH_2/dt \leq 3 \times 10^{-10}$ mol H_2/cm^2 min) are noticeably slower than initial values, appear relatively insensitive to material thickness, and are remarkably consistent when normalized for the contact area. The values were relatively constant over a three-year period and offer an alternative approach to the use of G values for estimating the extent of hydrogen generation, by avoiding difficulties in quantifying energy self-adsorption by the plutonium.

The uncertainty is somewhat reduced regarding the fate of hydrogen formed in plutonium-rich systems containing other materials. As expected, hydride formation does not occur if oxygen or water is present in high concentrations. However, the Pu + H_2 reaction occurred at a slow rate (on the order of 1×10^{-11} mol H_2/cm^2 min), during the tests with liquid alloys and MgO + H_2O slurry, after the concentrations of those species were reduced by their reaction with plutonium. Dichotomous hydriding behavior is encountered with systems containing hydrogenous materials. Hydrogen reacted in tests with Sylguard 184 and cellular silicone but accumulated in tests with ethylene glycol and silicone oil. A major difference between these materials is their mobility. The relevance of this factor is suggested by the large amounts of corrosion that occurred on convex surfaces compared with those that occurred on concave surfaces surrounding the test materials. Small differences are evident in the photographs of products from the tests with liquid alloy and MgO + H_2O slurry, but they are most pronounced for the tests with hydrogenous materials. Corrosion of plutonium by all species (O_2, H_2O and H_2) is apparently reduced in the immediate presence of hydrogenous material, an observation consistent with measurement of slow rates for the water catalyzed Pu + O_2 and the Pu + H_2O reactions in tests with hydrogenous materials. Whereas glycol and oil are mobile and were distributed over the entire plutonium surface, the potting compound and cellular polymer were confined to relatively small fractions of the metal surface. A reasonable conclusion is that hydriding did not occur in tests with glycol and silicone oil because essentially all plutonium surfaces were covered by or adjacent to those materials.

The occurrence of the hydride-catalyzed Pu + N_2 reaction in the absence of heat generation by the hydride-catalyzed Pu + O_2 has remained uncertain. However, results for the test with Sylguard 184 demonstrate that catalyzed nitriding proceeds at a measurable rate ($-dN_2/dt = 3.6 \times 10^{-10}$ mol H_2/cm^2 min) at 25°C, albeit orders of magnitude slower than observed in the presence of catalyzed oxidation [9]. Since the catalyzed reaction of N_2 with plutonium occurs via the reaction of nitrogen with surface hydride, these results also show that the PuH_2 + N_2

reaction occurs at room temperature. Nitriding was not observed during other tests in which hydride had formed, suggesting that the occurrence of the reaction is very unpredictable.

The present study provides important information about the compatibility of weapons-grade plutonium with differing types of chemical compounds and about the kinetics of gas generation in those systems. Both properties are of interest for assessing the potential consequences for the long-term storage of plutonium-containing materials. Liquid alloys were selected as unreactive reference substances. The formation of HCl in those systems demonstrates that trace impurities can have a large impact on behavior and on the suitability of storing plutonium-containing materials in stainless steel containers. However, the presence of moist air atmospheres in sealed containers composed of metal-rich materials appears to have no detrimental consequences. The internal pressure decreases as O_2 is consumed via the water-catalyzed cycle, increases as H_2 is formed by the Pu + H_2O reaction, and ultimately decreases as PuH_2 is formed by the Pu + H_2 reaction. After O_2 and H_2O are eliminated from the test systems, the behavior is like that expected for an inert atmosphere. Potential difficulties for long-term storage may arise if the rate of H_2 formation by the radiolysis of hydrogenous materials is rapid and the hydriding rate of plutonium is relatively slow.

A quantitative estimation of the pressure rise in a storage container is instructive. The most favorable storage configuration for a system containing plutonium and hydrogenous material is demonstrated by the test with Sylguard 184. The rate of pressure increase is minimized because the hydrogenous material is immobile and contact area with plutonium is limited. That configuration also appears to enhance the likelihood of hydriding at plutonium surfaces that are distant from the hydrogenous material. At the maximum H_2 generation rate (3×10^{-10} mol H_2/cm^2 of contact area min) observed for the silicone potting compound in contact with weapons-grade plutonium, the rate of pressure rise in a 1.0 liter volume is 3.0 torr/cm^2 of contact area *y*. Therefore, the anticipated pressure rise in a storage container with 2 liters of free volume and a contact area of 20 cm^2, over a 50 year period, is 750 torr. This pressure increase is modest, and the possibility of excessive pressurization is reduced by the likelihood of hydriding. However, similar calculations show that pressures on the order of 100 atm might be generated over that time period if the hydrogenous material is mobile (liquid or volatile), a large area of the plutonium surface is contacted, and H_2 accumulates.

Although the observations in this study are consistent and support the conclusions of this report, verification of the results at conditions of interest is recommended. Likewise, tests with other types of materials are desirable and expected to more accurately define factors relevant to extended storage of plutonium-containing materials.

References

1. J. M. Haschke and J. C. Martz, "Plutonium Storage," in *Encyclopedia of Environmental Analysis and Remediation*, R. A. Meyers, Ed., Vol. 6, John Wiley and Sons, Inc., New York, 1998, pp. 3740–3755.

2. "Criteria for Preparing and Packaging Plutonium Metals and Oxides for Long-Term Storage," Department of Energy Standard DOE-STD-3013, US Department of Energy, Washington, DC, September 1996.

3. J. M. Haschke and T. H. Allen, "Interactions of Plutonium Dioxide with Water and Oxygen-Hydrogen Mixtures," Los Alamos National Laboratory report LA-13537-MS, Los Alamos, New Mexico, January 1999.

4. G. Friedlander, J. W. Kennedy, and J. M. Miller, *Nuclear and Radiochemistry*, Second Edition, John Wiley and Sons, Inc., New York, 1964, Chap. 4.

5. J. M. Haschke, T. H. Allen, and J. L. Stakebake, J. Alloys Comp., **243** (1996) 23.

6. J. L. Stakebake and M. A. Saba, J. Less-Common Metals, **158** (1990) 221.

7. J. L. Stakebake and L. A. Lewis, J. Less-Common Metals, **136** (1988) 349.

8. J. M. Haschke, T. H. Allen, and L. A. Morales, "Surface and Corrosion Chemistry of Plutonium," Los Alamos Science, **26** (1999) in press.

9. J. M. Haschke, T. H. Allen, and J. C. Martz, J. Alloys Comp., **271-273** (1998) 211.

10. J. M. Haschke, A. E. Hodges, G. E. Bixby, and R. L. Lucas, "The Reaction of Plutonium with Water: Kinetic and Equilibrium Behavior of Binary and Ternary Phases in the Pu+O+H System," Rocky Flats report RFP-3416, Rockwell International, Rocky Flats Plant, Golden, Colorado, February 1983.

11. J. M. Haschke, “Hydrolysis of Plutonium: The Plutonium-Oxygen Phase Diagram,” in *Transuranium Elements A Half Century*, L. R. Morss and J. Fuger, Eds., American Chemical Society, Washington, DC, 1992.

12. J. M. Haschke, T. H. Allen, L. A. Morales, D. M. Jarboe, and C. V. Puglisi, “Chloride-Catalyzed Corrosion of Plutonium in Glovebox Atmospheres,” Los Alamos National Laboratory report LA-13428-MS, Los Alamos, New Mexico, April 1998.

13. J. C. Martz, J. M. Haschke, and J. L. Stakebake, J. Nucl. Mater., **210** (1994) 130.

Appendices

Contents

Appendix A: Initial and final photographs of the test with $MgO + H_2O$ + ethylene glycol

Appendix B: Initial and final photographs of the test with $MgO + H_2O$

Appendix C: Initial and final photographs of the test with silicone oil

Appendix D: Initial and final photographs of the test with cellular silicone

Appendix E: Initial and final photographs of the test with Sylguard 184

Appendix F: Initial and final photographs of the test with Indalloy 51

Appendix G: Initial and final photographs of the test with Indalloy 51 + copper powder

Appendix A
MgO + H_2O + Ethylene Glycol

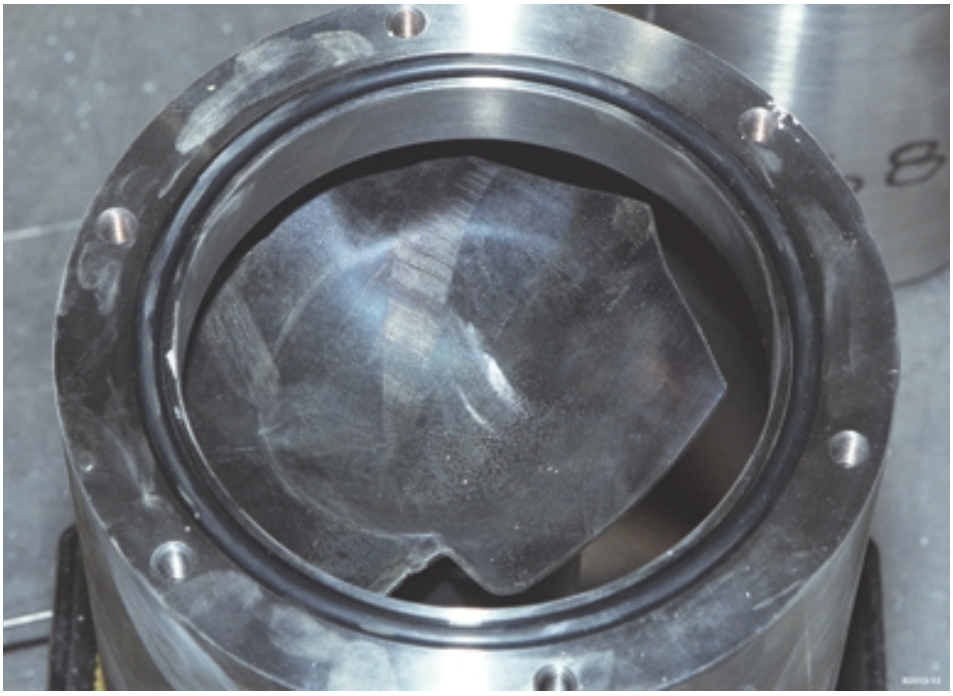

1. Plutonium specimen before the test.

2. MgO + H_2O + ethylene glycol slurry in the plutonium cup before the test.

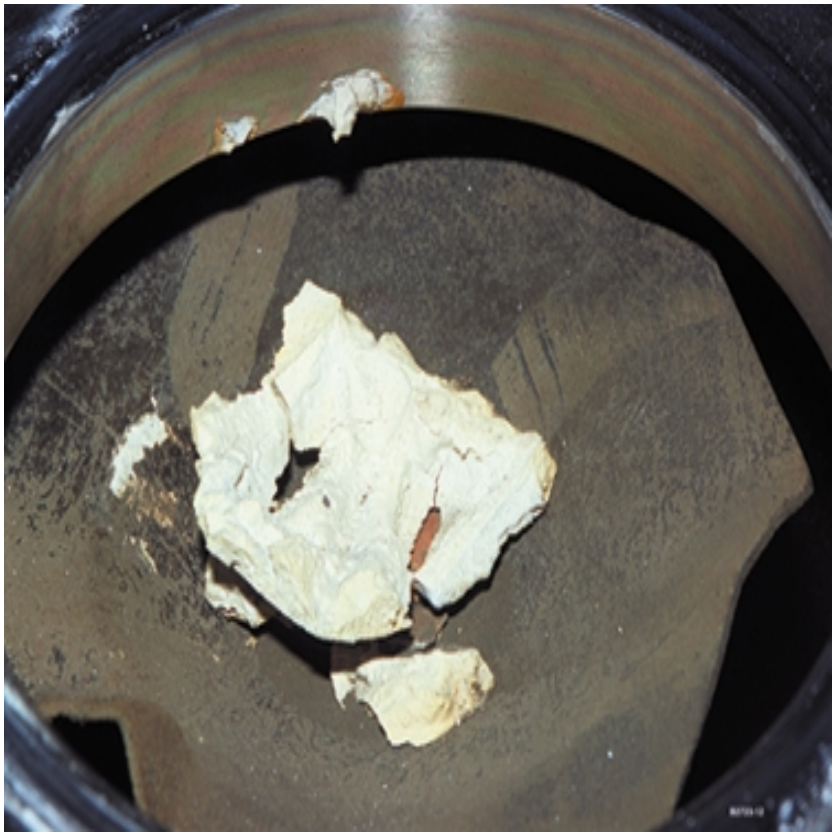

3. Residual test material and adjacent plutonium surface after the test.

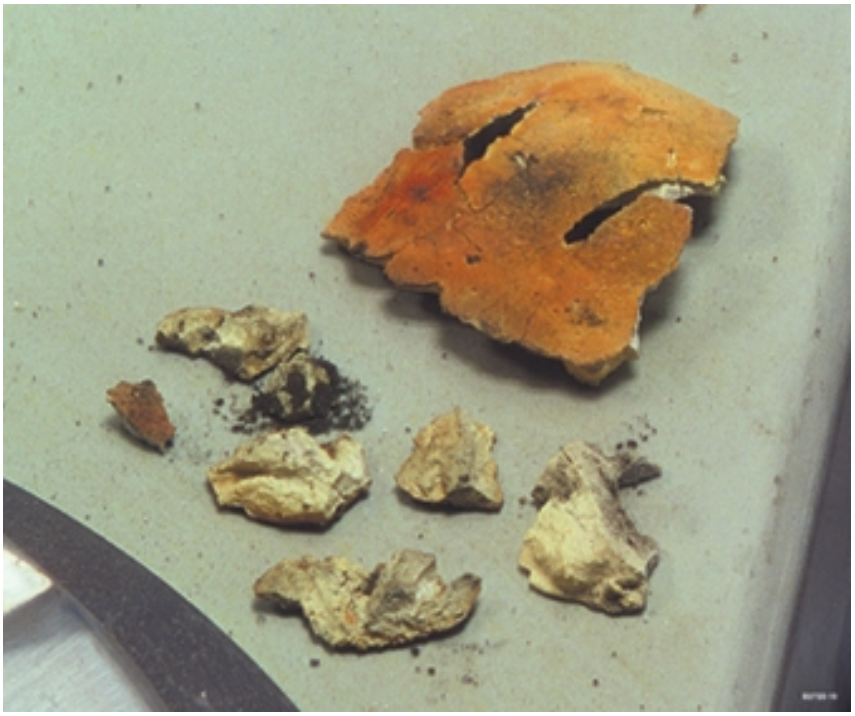

4. Contact surface of the residual test material after the test.

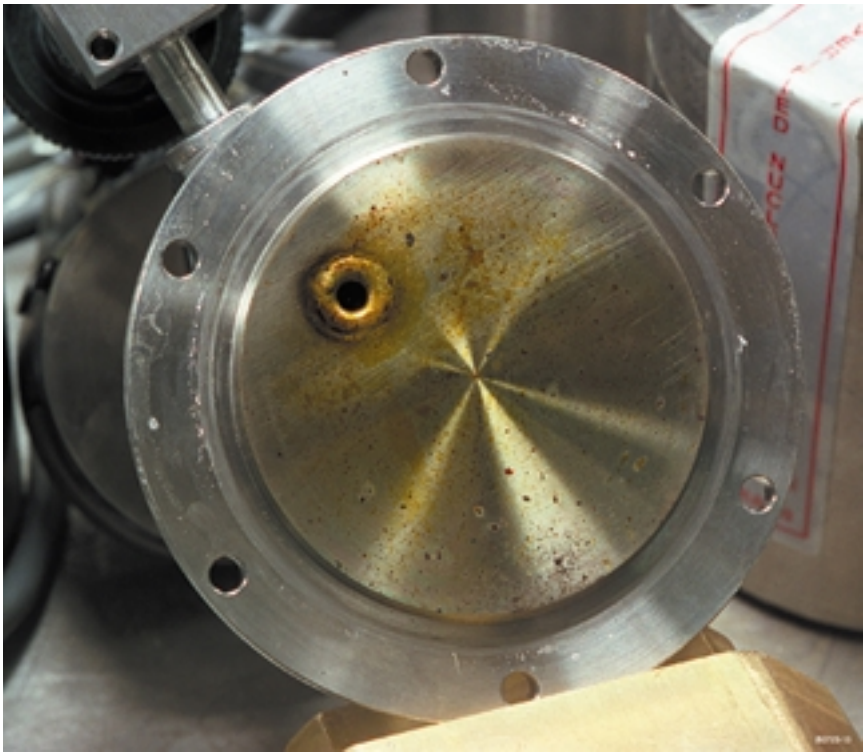

5. Varnish-like deposit on reactor lid above the specimen after the test.

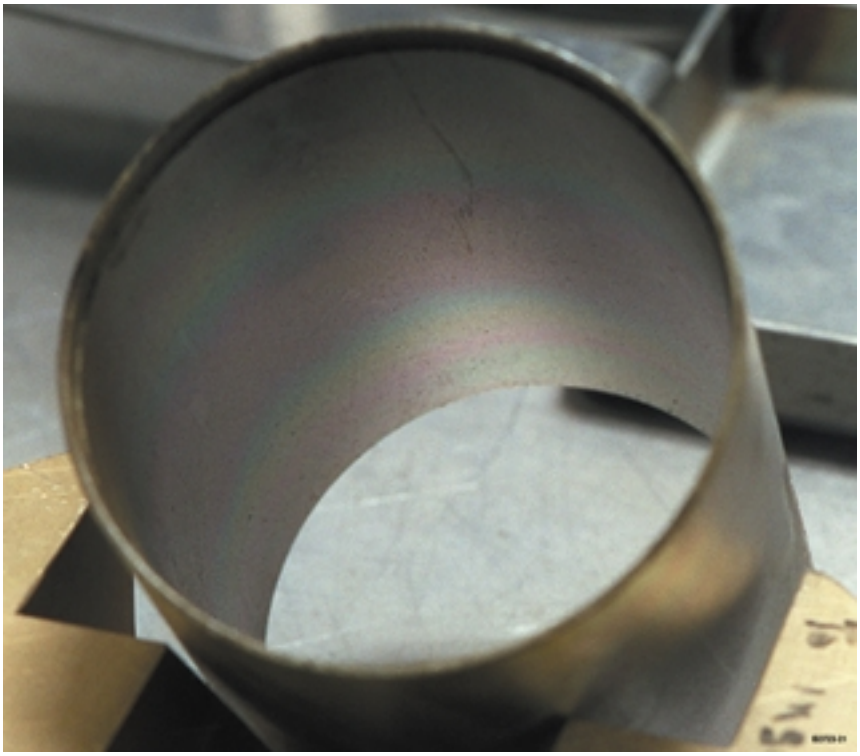

6. Layer of varnish-like deposit on the inside of the stainless steel stand after the test.

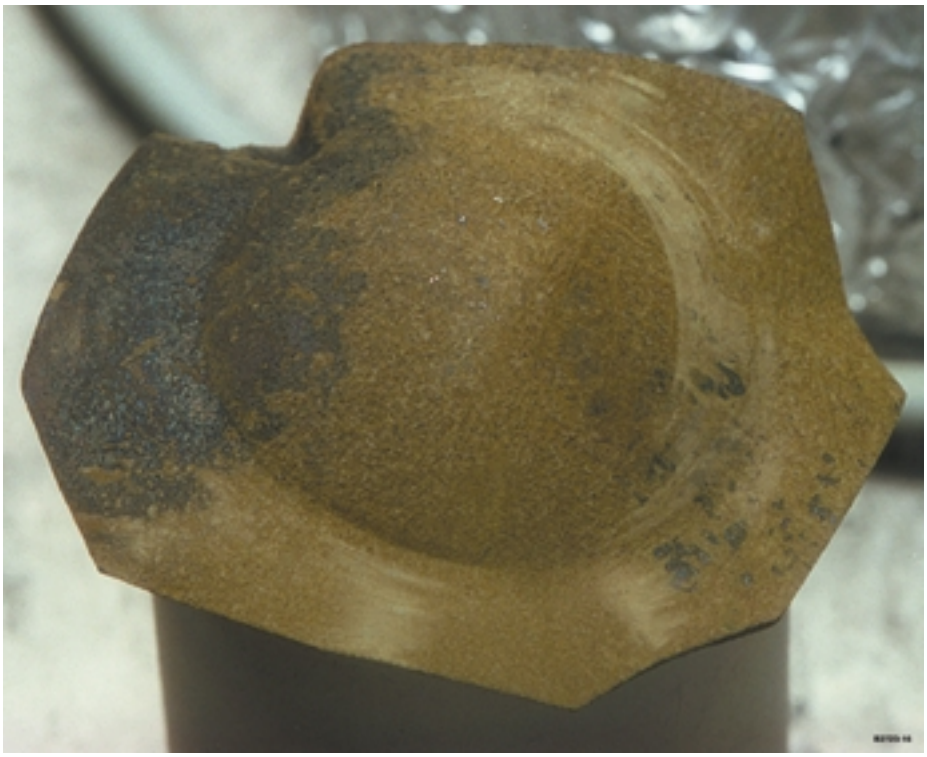

7. Convex surface of the plutonium specimen after the test.

Appendix B
$MgO + H_2O$

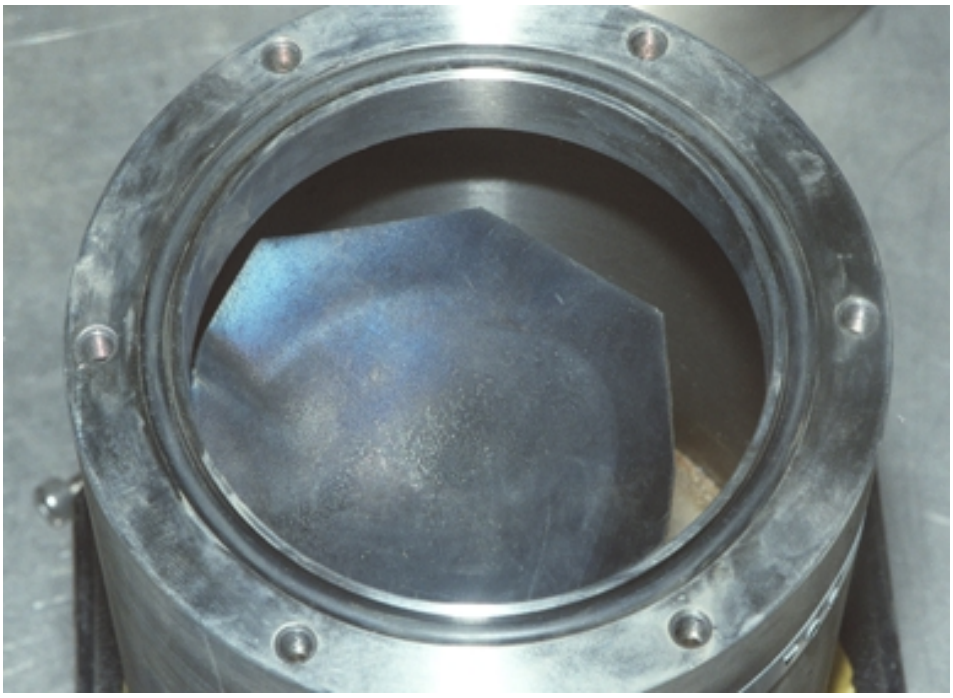

1. Plutonium specimen before the test.

2. $MgO + H_2O$ slurry in the plutonium cup before the test.

3. Residual test material and adjacent plutonium surface after the test.

4. Contact surface of the residual test material after the test.

5. Concave surface of the plutonium specimen after the test.

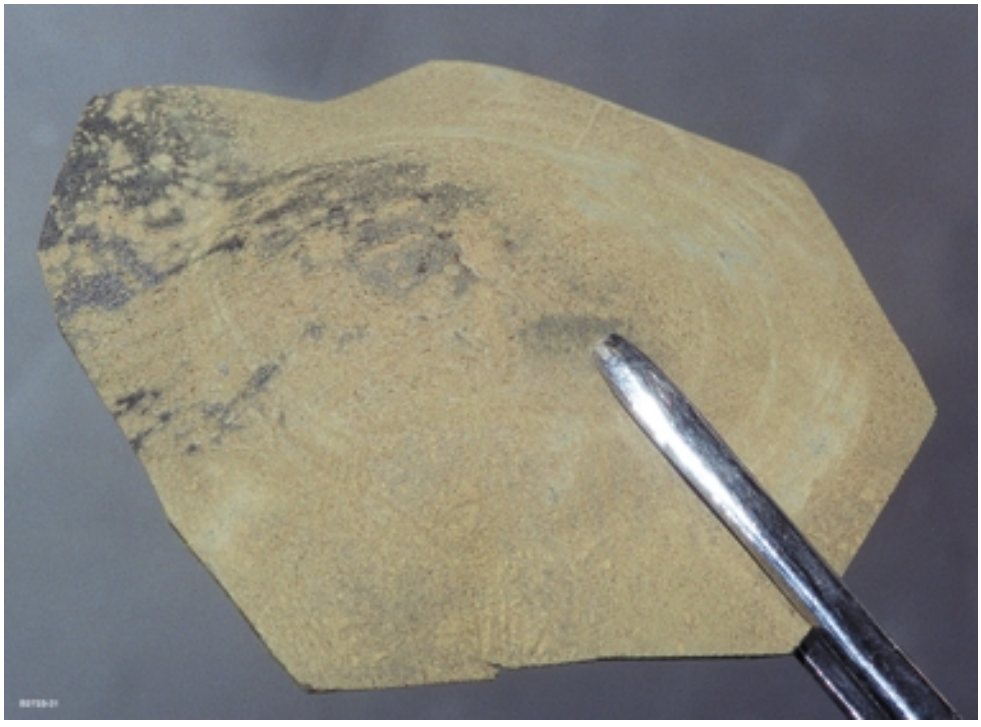

6. Convex surface of the plutonium specimen after the test.

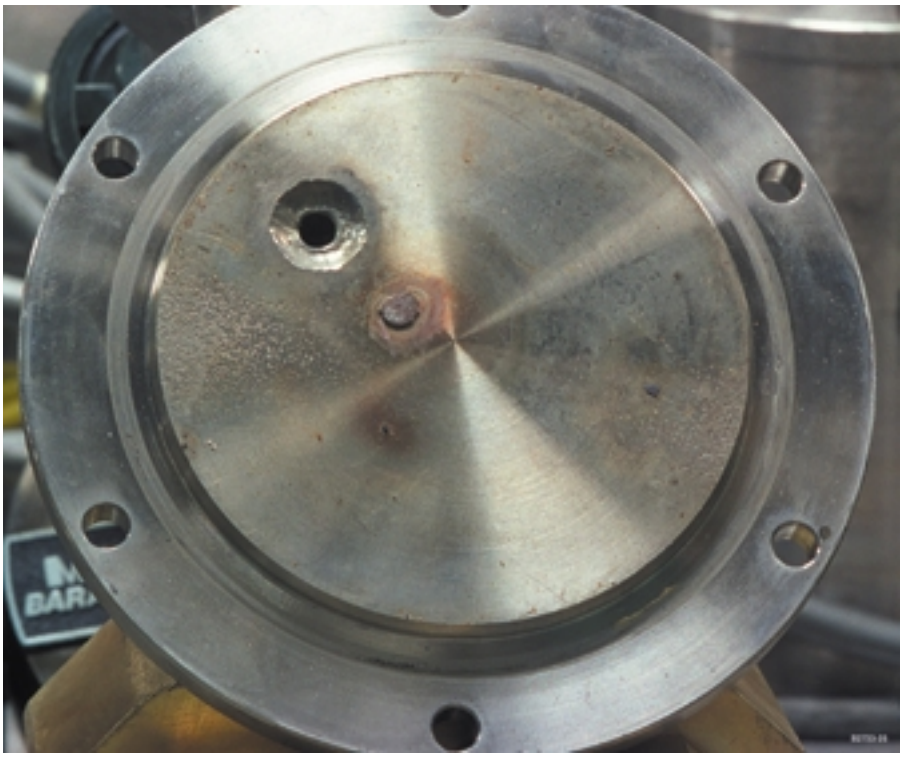

7. Unidentified deposit on the reactor lid after the test.

Appendix C
Silicone Oil

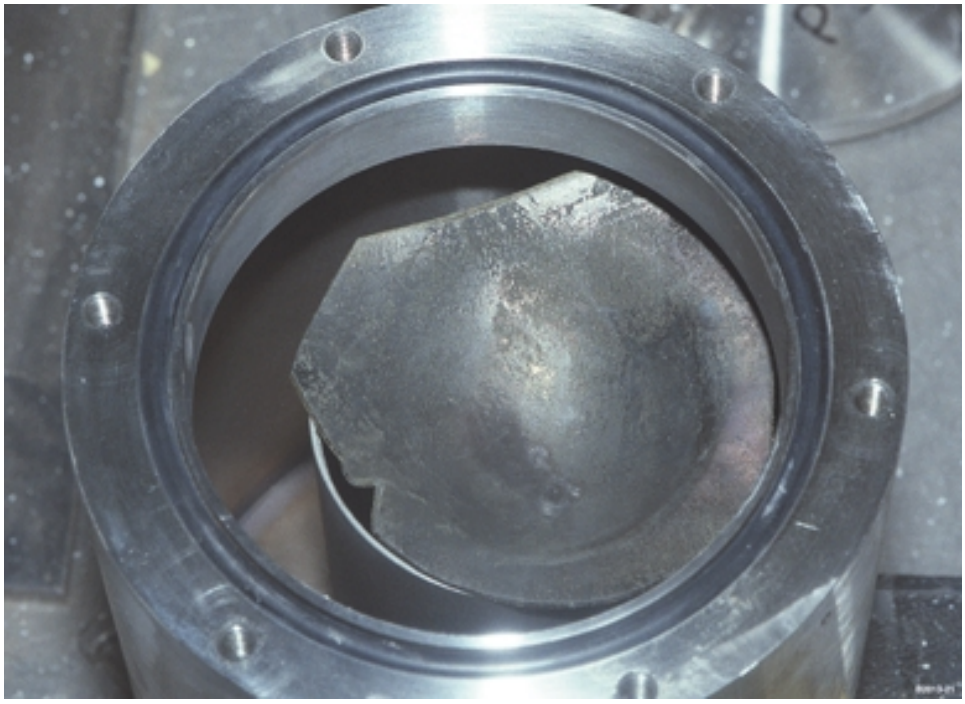

1. Plutonium specimen before the test.

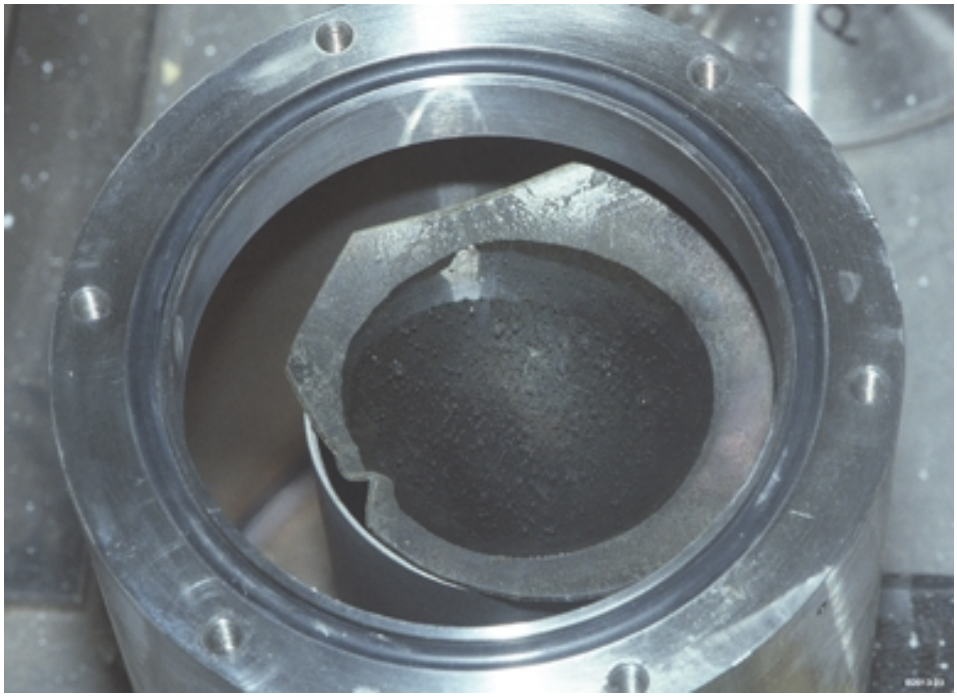

2. Silicone oil in the plutonium cup before the test.

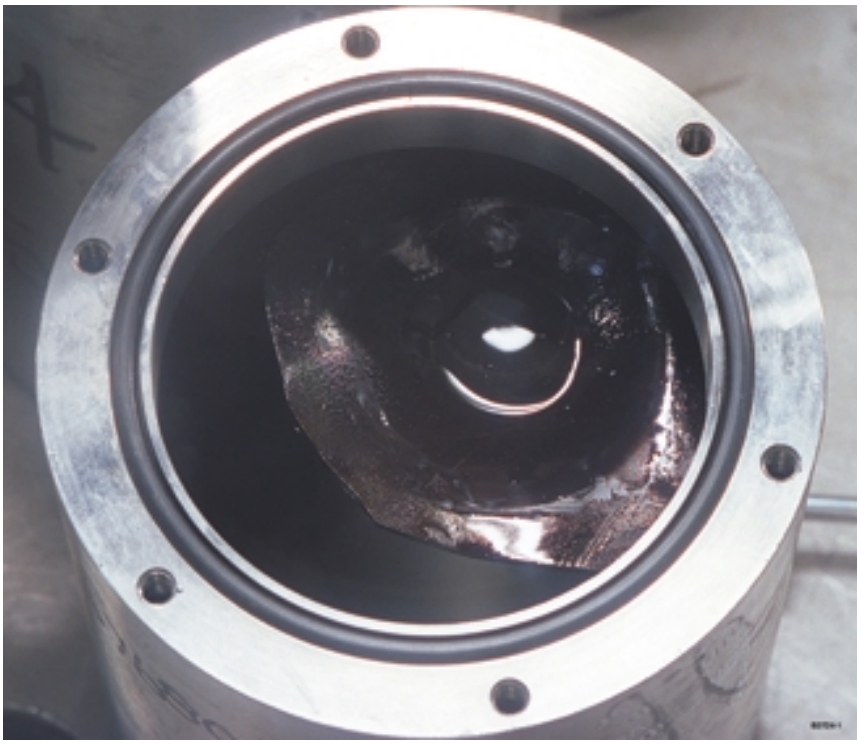

3. Residual test material in plutonium cup after the test.

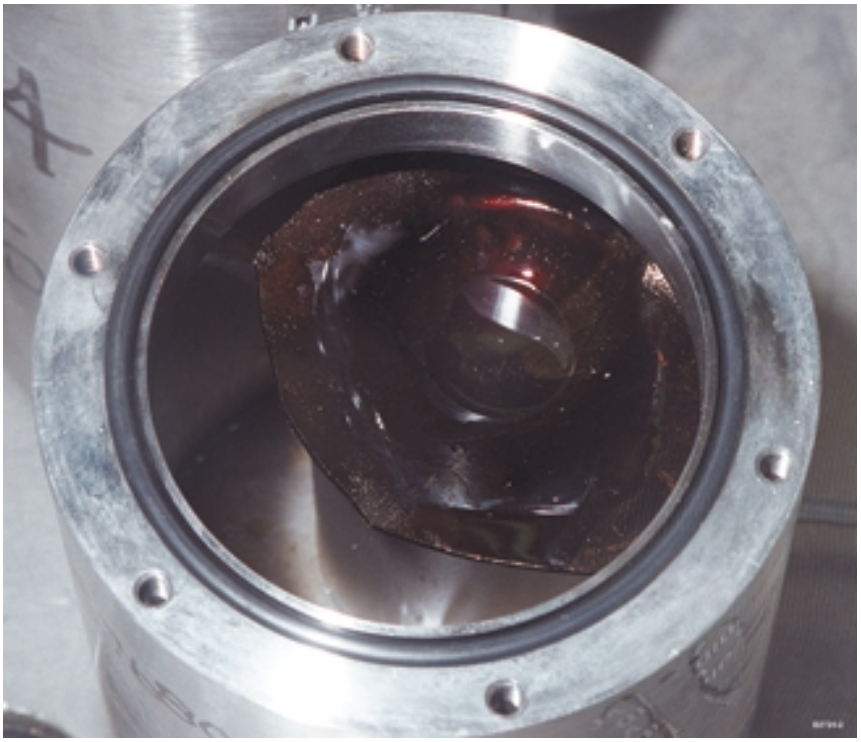

4. Viscous test material with the plutonium cup in a vertical position after the test.

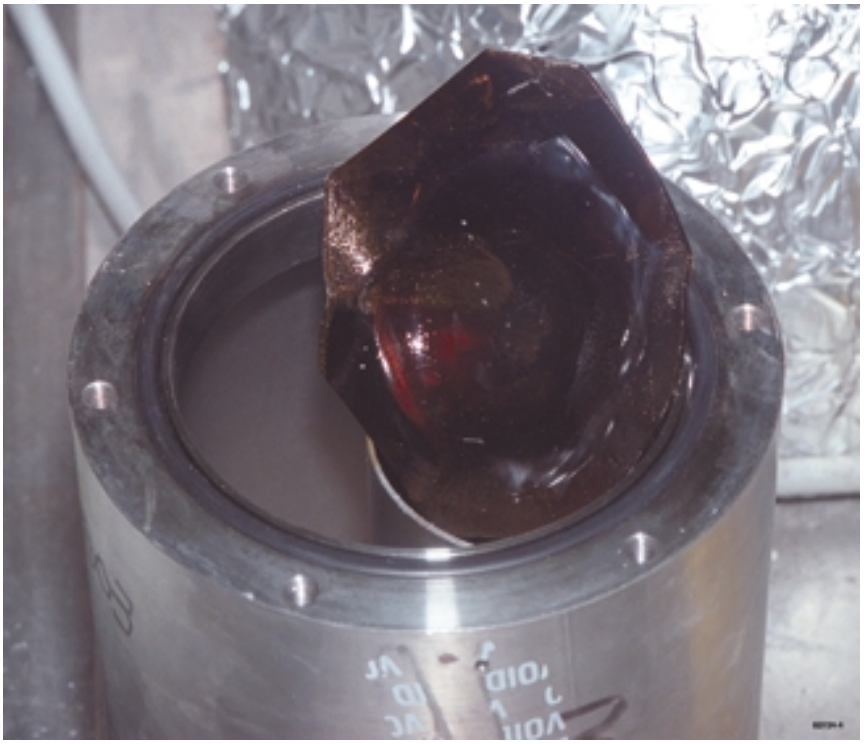

5. Concave surface of the plutonium specimen after the test.

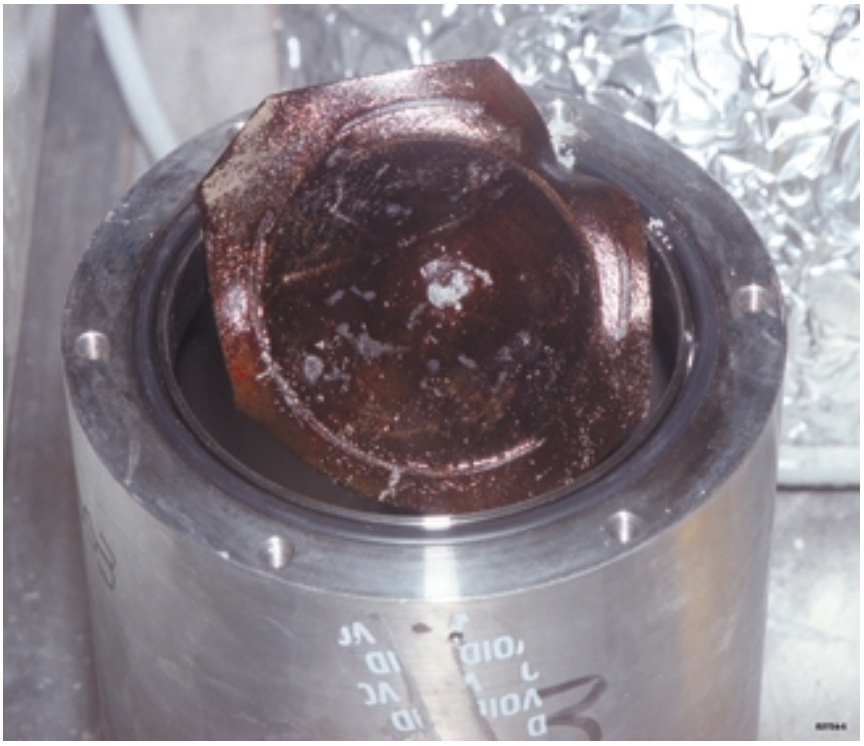

6. Areas of corrosion on convex surface of the plutonium specimen after the tests.

Appendix D
Cellular Silicone

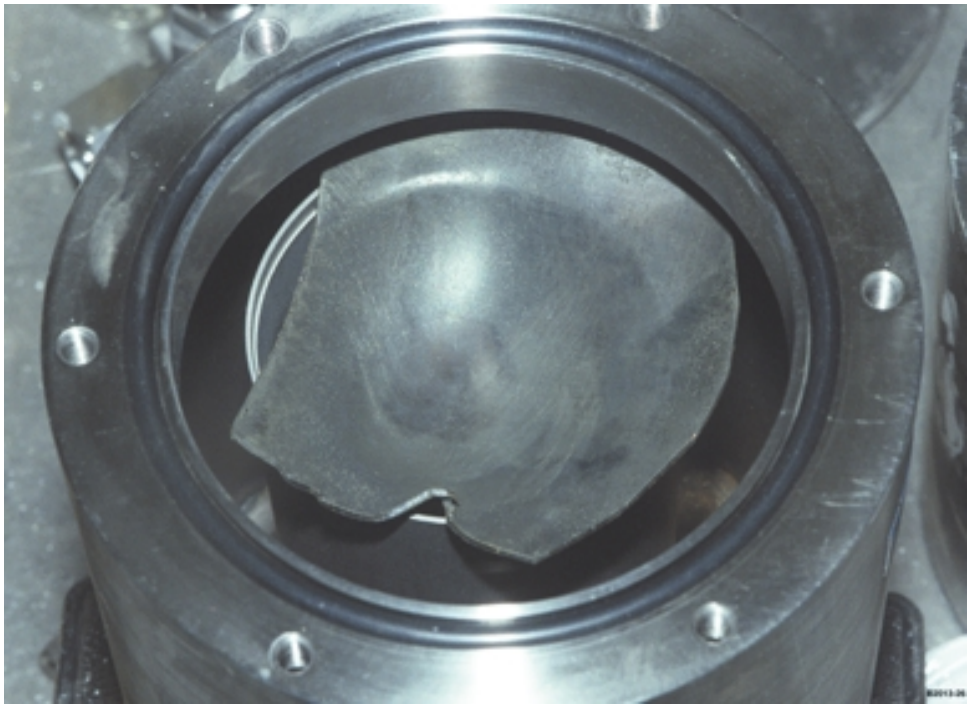

1. Plutonium specimen before the test.

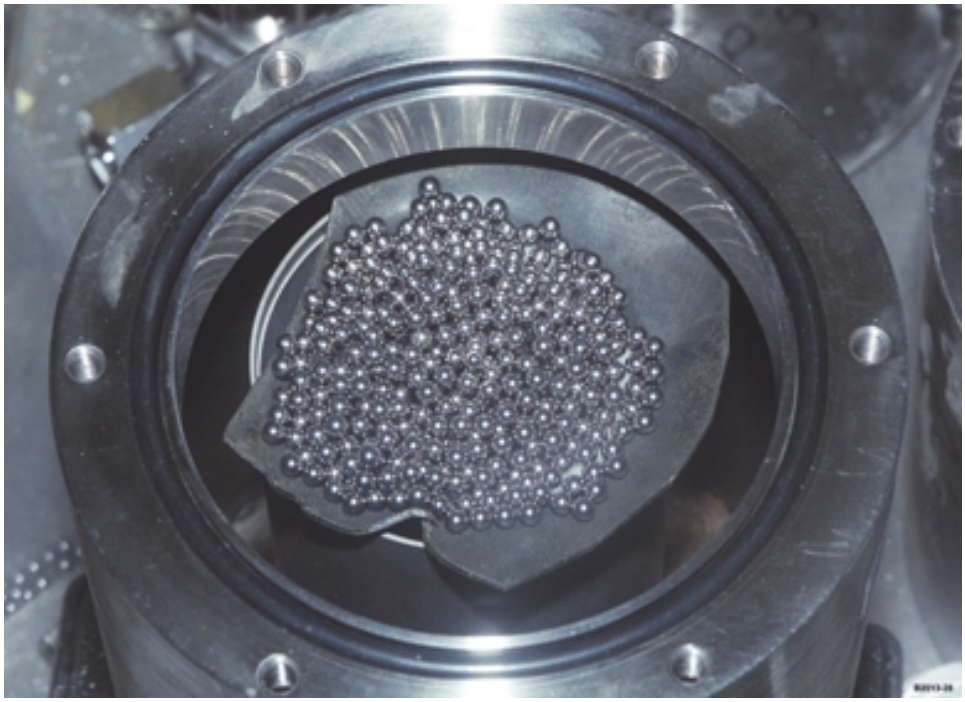

2. Cellular silicone in the plutonium cup beneath stainless steel shot before the test.

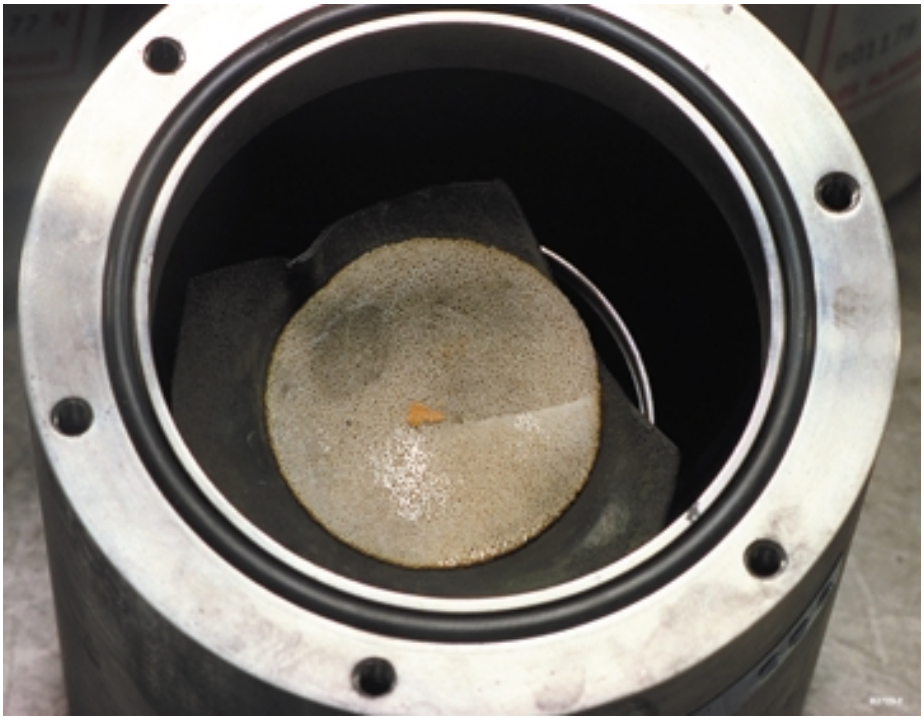

3. Upper surface of test material after the test.

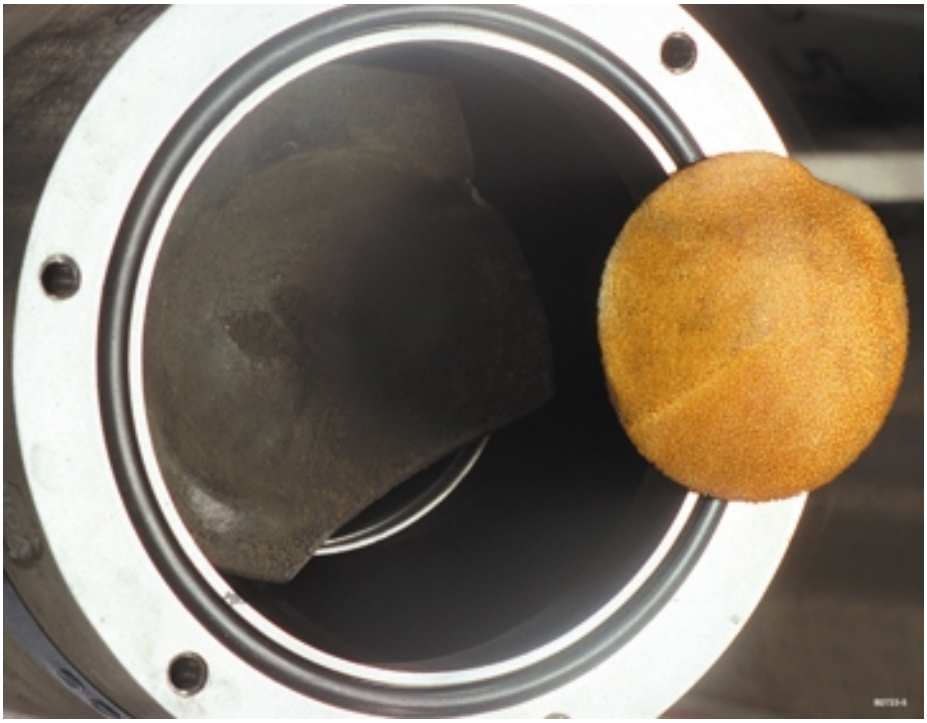

4. Contact surface of the residual test material and surrounding plutonium surface after the test.

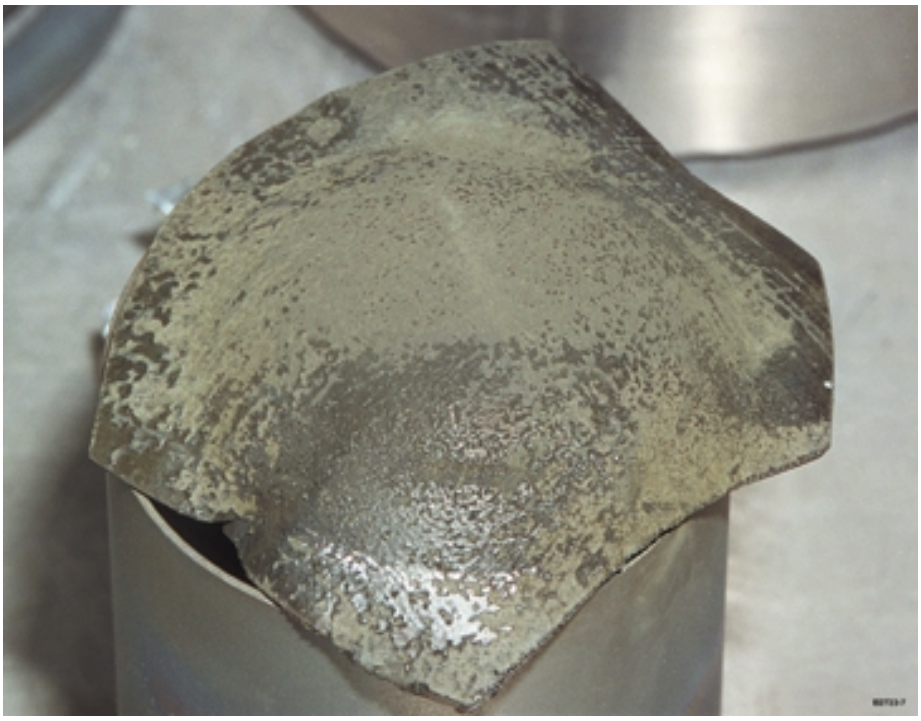

5. Convex surface of the plutonium specimen after the test.

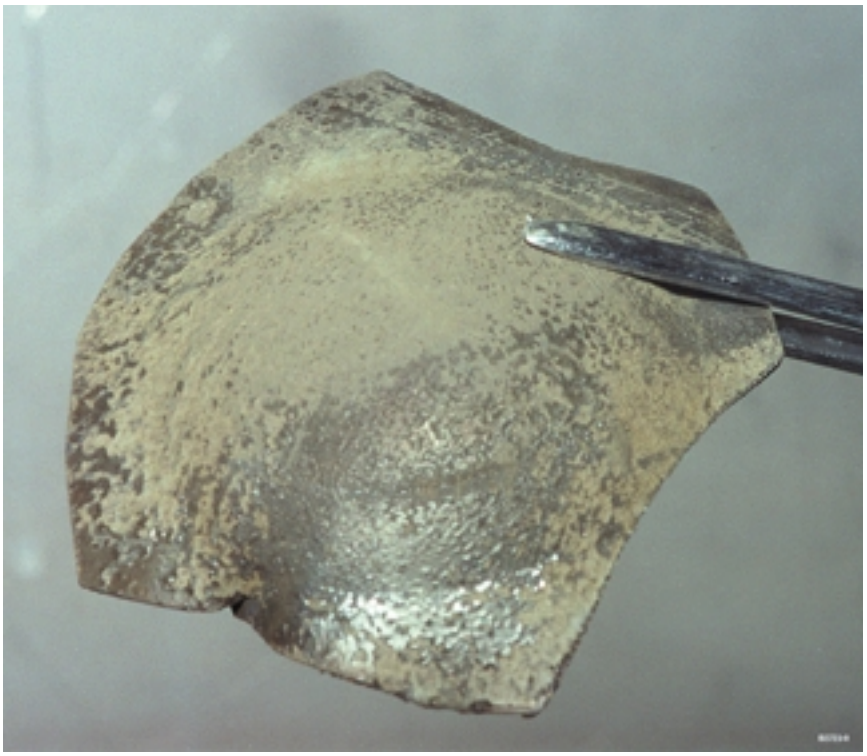

6. Alternate view of convex surface of the plutonium specimen after the test.

Appendix E
Sylguard 184

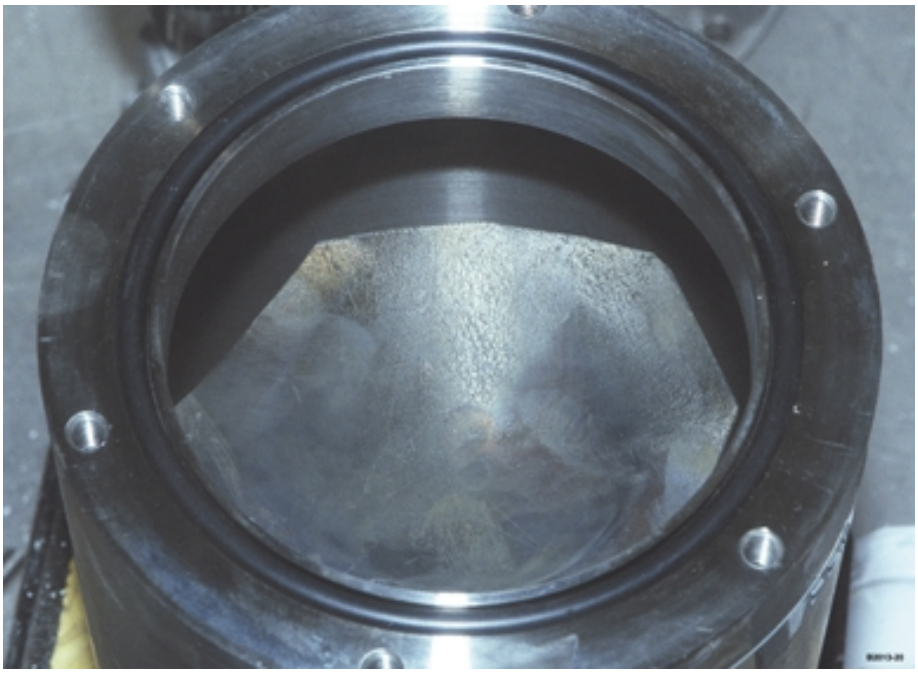

1. Plutonium specimen before the test (photographs of the test material were not taken).

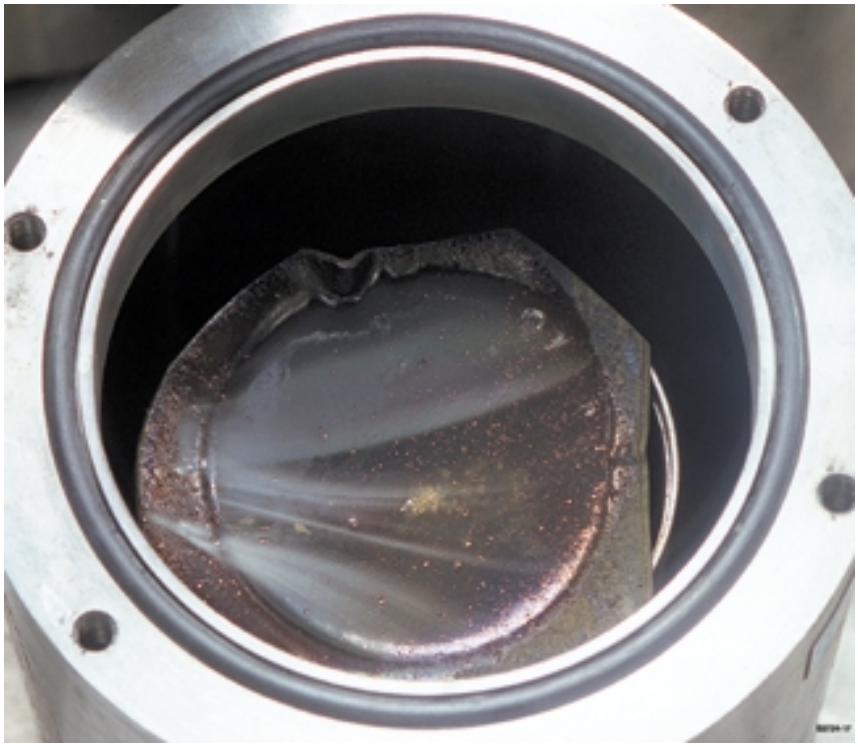

2. Residual test material in plutonium cup after the test.

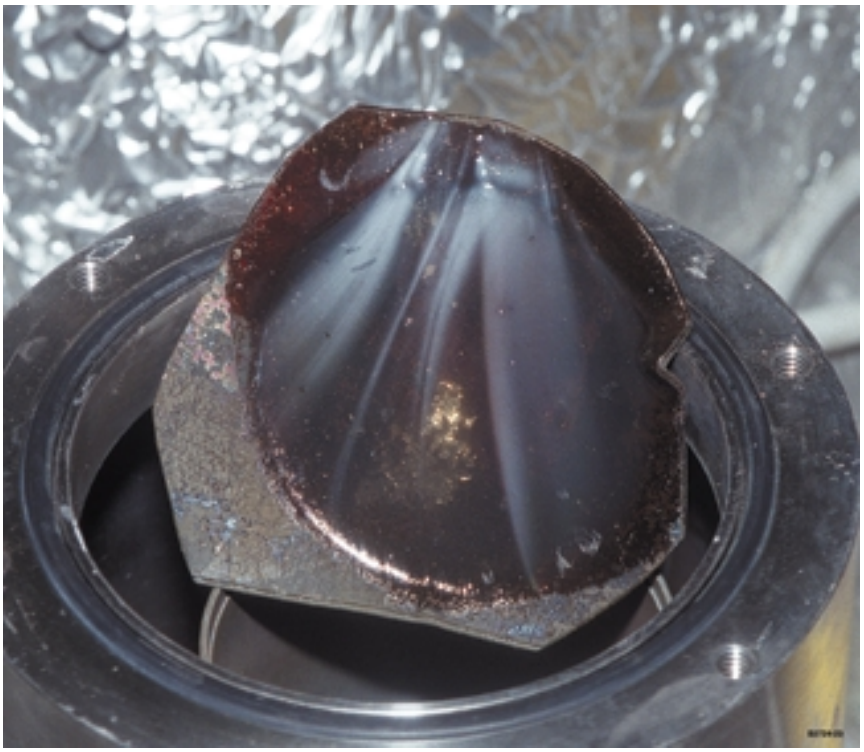

3. Alternate view of residual test material in plutonium cup after the test.

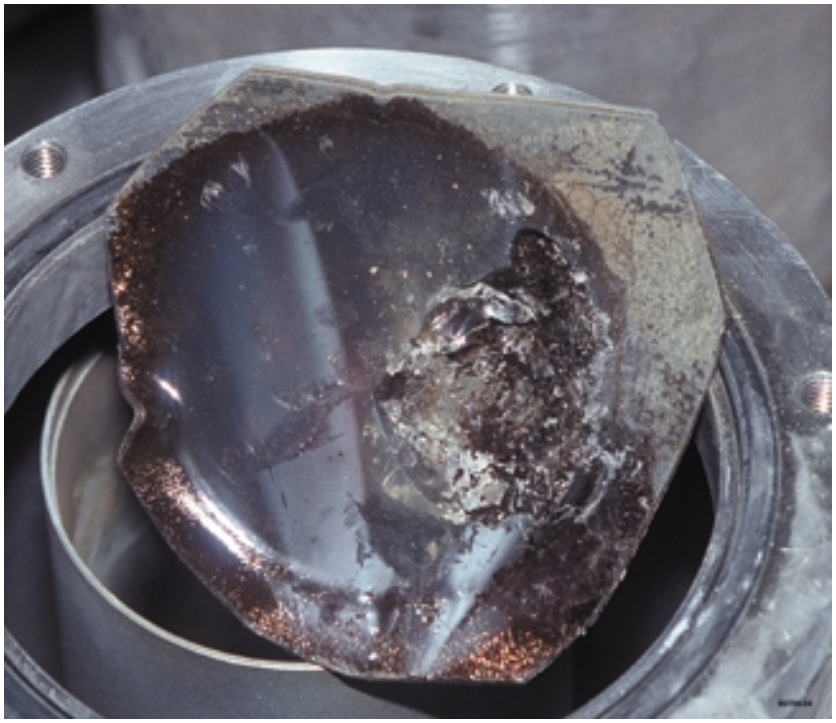

4. Residual test material after an attempt was made to remove it from the plutonium cup.

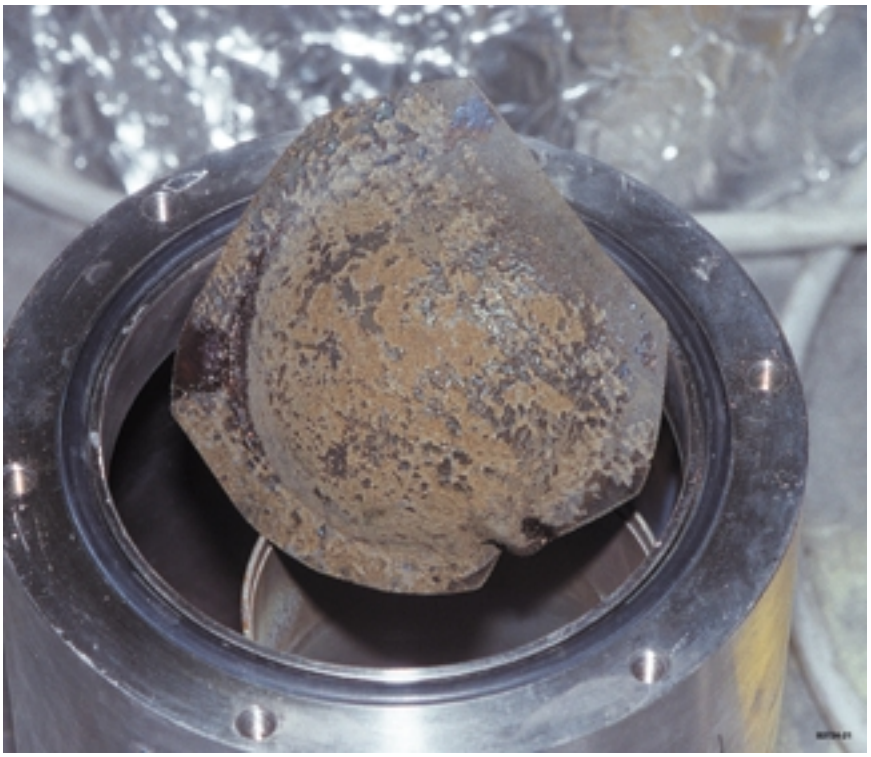

5. Convex surface of the plutonium specimen after the test.

Appendix F
Indalloy 51

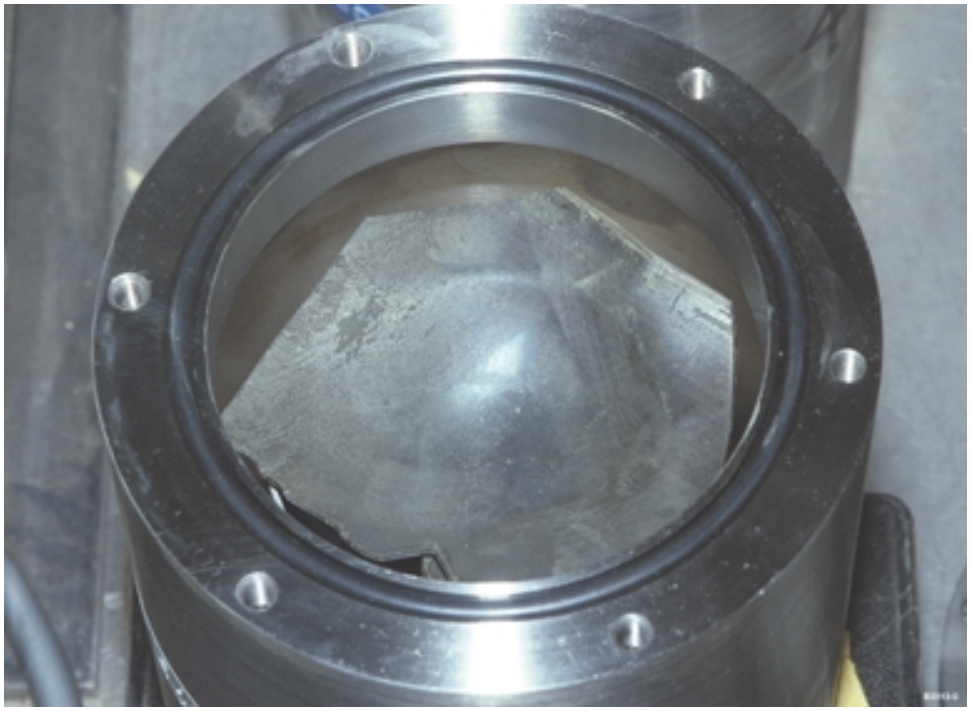

1. Plutonium specimen before the test.

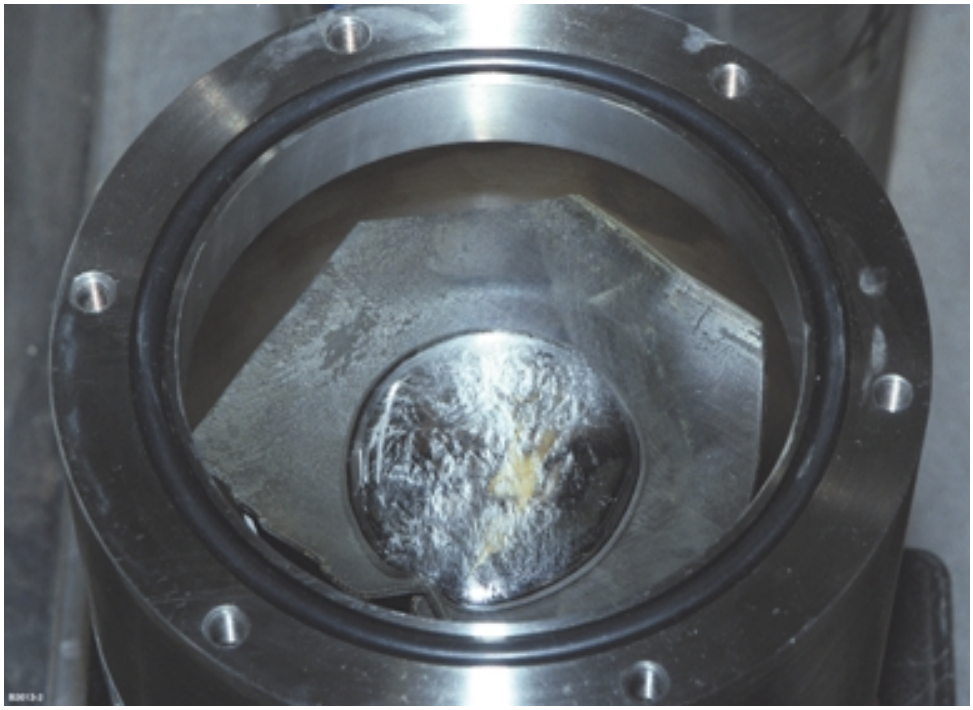

2. Liquid Indalloy 51 alloy in the plutonium cup before the test.

3. Solid residual test material in the plutonium cup and adjacent plutonium surface after the test.

4. Liquid Indalloy 51 in reactor with powdered corrosion product after the test.

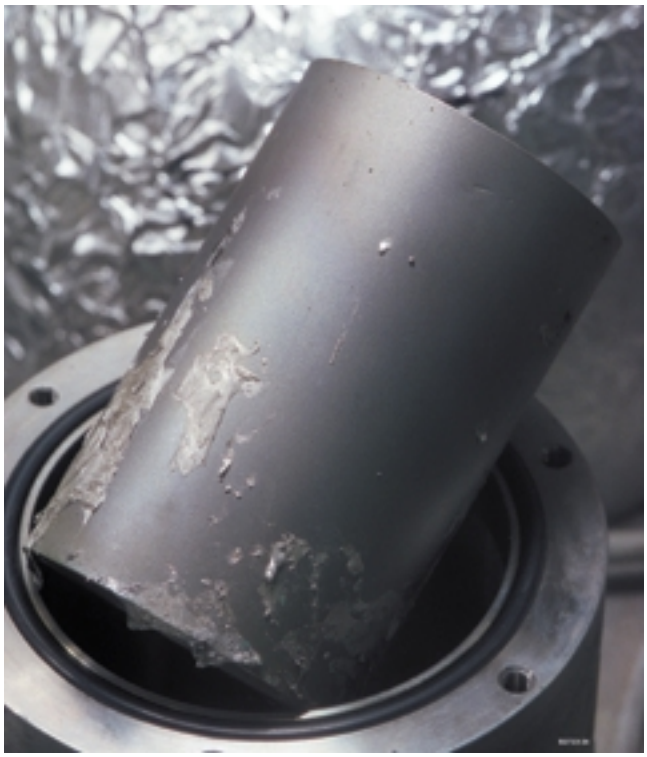

5. Indalloy 51 adhering to the stainless steel specimen stand after the test.

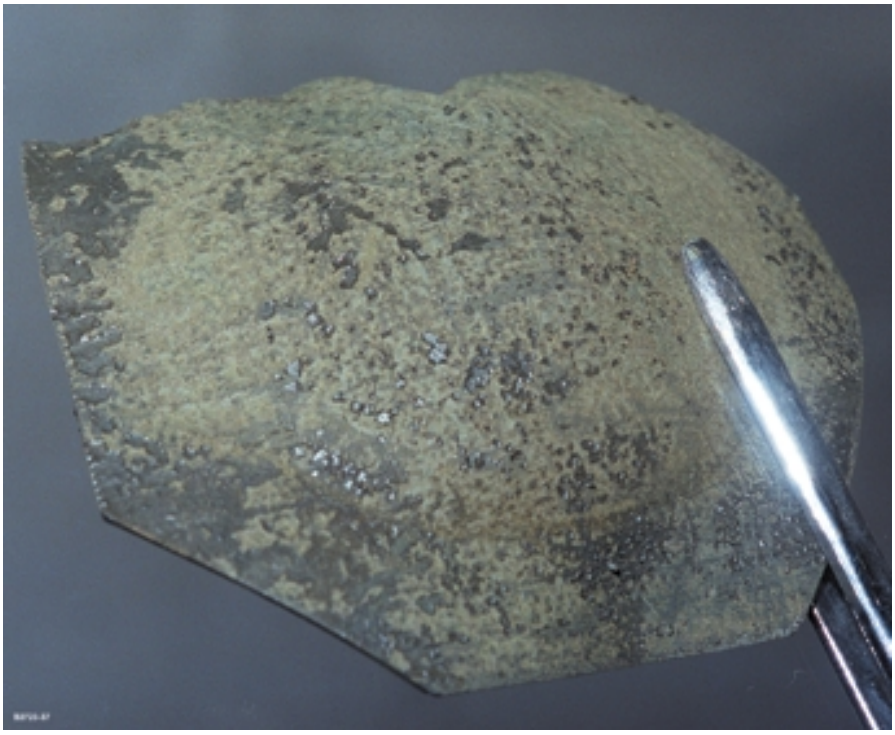

6. Convex surface of the plutonium specimen after the test.

Appendix G
Indalloy 51 + copper powder

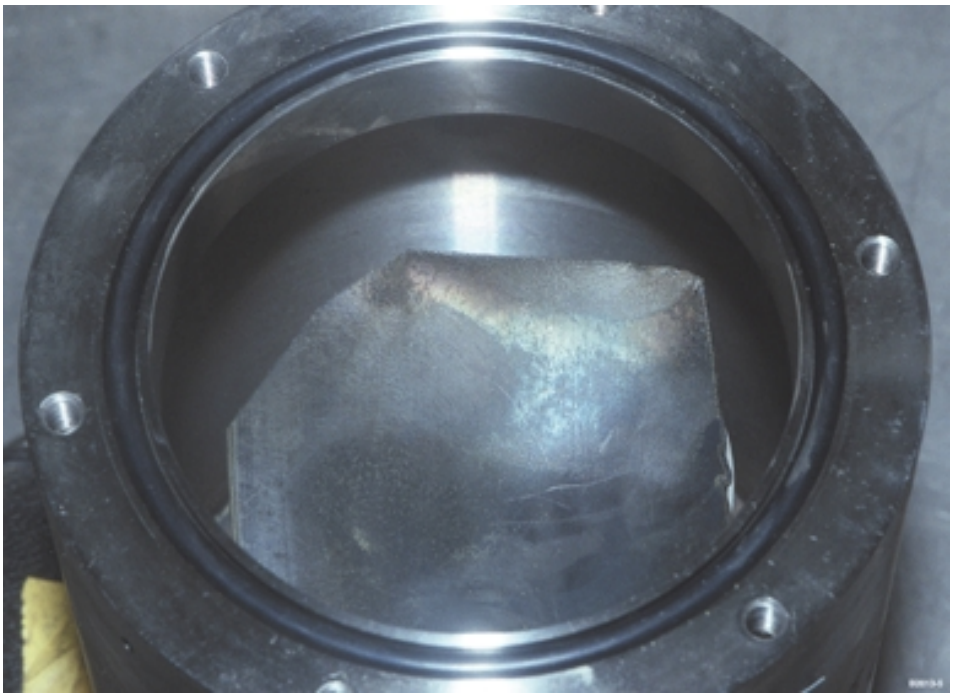

1. Plutonium specimen before the test.

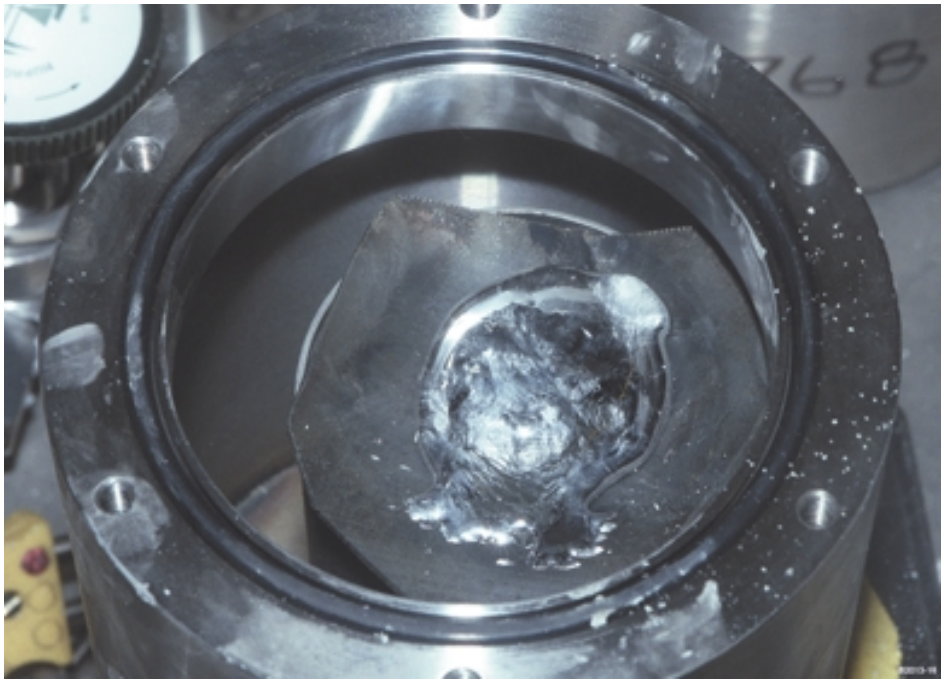

2. Mixture of Indalloy 51 + copper powder alloy in the plutonium cup before the test.

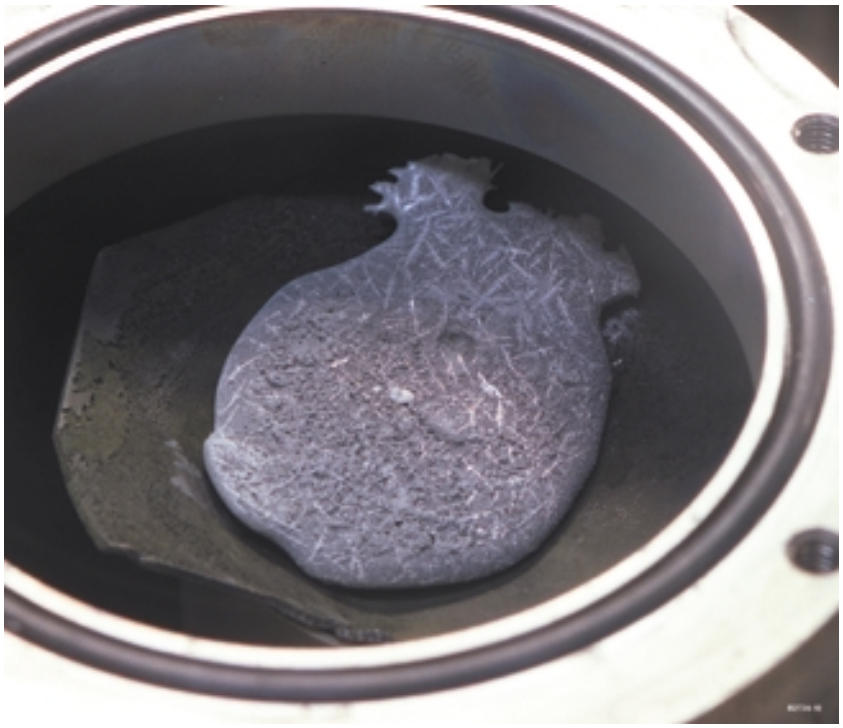

3. Solid residual test material in the plutonium cup and adjacent plutonium surface after the test.

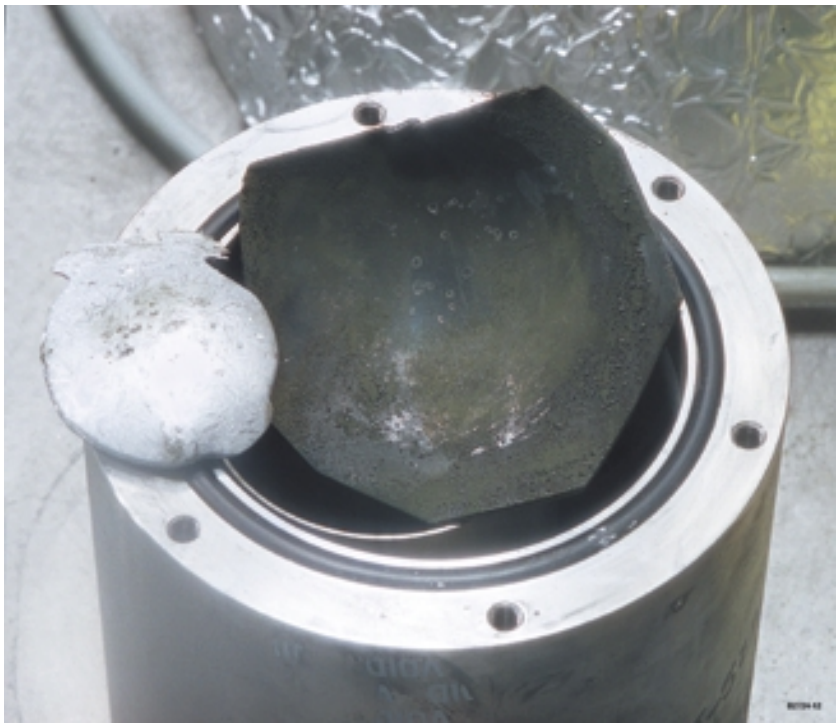

4. Contact surface of test material and the surface of the plutonium cup after the test.

5. Convex surface of the plutonium specimen after the test.

Los Alamos
NATIONAL LABORATORY
Los Alamos, New Mexico 87545